Adipocyte Glucocorticoid Receptor Activation With High Glucocorticoid Doses Impairs Healthy Adipose Tissue Expansion by Repressing Angiogenesis

Anna Vali, Héloïse Dalle, Alya Loubaresse, Jérôme Gilleron, Emmanuelle Havis, Marie Garcia, Carine Beaupère, Clémentine Denis, Natacha Roblot, Karine Poussin, et al.

American Diabetes Association. diabetes

Adipocyte glucocorticoid receptor impairs adipose tissue healthy expansion through repression of angiogenesis

Journal:	*Diabetes*
Manuscript ID	Draft
Manuscript Type:	Original Article: Metabolism
Date Submitted by the Author:	n/a
Complete List of Authors:	Vali, Anna; Sorbonne Université, Inserm, Centre de Recherche Saint-Antoine, CRSA, Metabolism Inflammation; Sorbonne Université, Inserm, Institute of CardioMetabolism and Nutrition, ICAN Dalle, Héloïse; Sorbonne Université, Inserm, Centre de Recherche Saint-Antoine, CRSA, Metabolism Inflammation; Sorbonne Université, Inserm, Institute of CardioMetabolism and Nutrition, ICAN, Metabolism Inflammation Gilleron, Jérôme; INSERM U1065, C3M, Cellular and Molecular Physiopathology of Obesity Havis, Emmanuelle; CNRS-SU UMR 7622 INSERM ERL U1156, Institut Biologie Paris Seine (IBPS) Garcia, Marie; Sorbonne Université, Inserm, Centre de Recherche Saint-Antoine, CRSA, Metabolism Inflammation; Sorbonne Université, Inserm, Institute of CardioMetabolism and Nutrition, ICAN Beaupere, Carine; Sorbonne Université, Inserm, Centre de Recherche Saint-Antoine, CRSA, Metabolism Inflammation; Sorbonne Université, Inserm, Institute of CardioMetabolism and Nutrition, ICAN Denis, Clémentine; Sorbonne Université, Inserm, Centre de Recherche Saint-Antoine, CRSA, Metabolism Inflammation; Sorbonne Université, Inserm, Institute of CardioMetabolism and Nutrition, ICAN Roblot, Natacha; Sorbonne Université, Inserm, Centre de Recherche Saint-Antoine, CRSA, Metabolism Inflammation; Sorbonne Université, Inserm, Institute of CardioMetabolism and Nutrition, ICAN Poussin, Karine; Sorbonne Université, Inserm, Centre de Recherche Saint-Antoine, CRSA, Metabolism Inflammation; Sorbonne Université, Inserm, Institute of CardioMetabolism and Nutrition, ICAN Ledent, Tatiana; Sorbonne Université, Inserm, Centre de Recherche Saint-Antoine, CRSA, Metabolism Inflammation Bouillet, Benjamin; CHU Dijon , Service Endocrinologie, Diabetologie, Maladies Métaboliques Cormont, Mireille; INSERM U1065, C3M, Cellular and Molecular Physiopathology of Obesity Tanti, Jean-Francois; Batiment Universitaire Archimed, INSERM U895 Capeau, Jacqueline; UPMC, Inserm, Centre de Recherche Saint-Antoine Vatier, Camille; INSERM, UMR_S938, Centre de Recherche Saint-Antoine Fève, Bruno; Sorbonne Université, Inserm, Institute of CardioMetabolism and Nutrition, ICAN; Sorbonne Université, Inserm, Centre de Recherche Saint-Antoine, CRSA, AP-HP, Hôpital Saint-Antoine, Service Endocrinologie, CRMR PRISIS

	Grosfeld, Alexandra; Sorbonne Université, Inserm, Centre de Recherche Saint-Antoine, CRSA, Metabolism Inflammation; Sorbonne Université, Inserm, Institute of CardioMetabolism and Nutrition, ICAN Moldes, Marthe; Sorbonne Université, Inserm, Centre de Recherche Saint-Antoine, CRSA, Metabolism Inflammation; Sorbonne Université, Inserm, Institute of CardioMetabolism and Nutrition, ICAN

Adipocyte glucocorticoid receptor impairs adipose tissue healthy expansion through repression of angiogenesis

Anna Vali[1,2], Héloïse Dalle[1,2], Jérôme Gilleron[3], Emmanuelle Havis[4], Marie Garcia[1,2], Carine Beaupère[1,2], Clémentine Denis[1,2], Natacha Roblot[1,2], Karine Poussin[1,2], Tatiana Ledent[1], Benjamin Bouillet[1,2], Mireille Cormont[3], Jean-François Tanti[3], Jacqueline Capeau[1,2], Camille Vatier[2,5], Bruno Fève[2,5]*, Alexandra Grosfeld[1,2]*, Marthe Moldes[1,2#]

Affiliations

[1]Sorbonne Université, Inserm, Centre de Recherche Saint-Antoine, CRSA, F-75012 Paris, France

[2]Sorbonne Université, Inserm, Institute of CardioMetabolism and Nutrition, ICAN, F-75013 Paris, France

[3]Université Côte d'Azur, Inserm, C3M, Team Cellular and Molecular Pathophysiology of Obesity, Nice, France

[4]Sorbonne Université, CNRS, Inserm, Laboratoire de Biologie du Développement, Institut Biologie Paris Seine, IBPS, F75005 Paris, France

[5]Sorbonne Université, Inserm, Centre de Recherche Saint-Antoine, CRSA, AP-HP, Hôpital Saint-Antoine, Service Endocrinologie, CRMR PRISIS, 75012 Paris, France

*These authors contributed equally.

[#]Corresponding author: Marthe Moldes, Centre de Recherche Saint-Antoine, Sorbonne Université, Inserm UMR_S938, 27 rue de Chaligny, 75012 Paris, France, Phone number : +33140011355 ; Email : marthe.moldes@inserm.fr

Keywords: Adipose tissue, glucocorticoid receptor, angiogenesis, VEGFA, HIF-1a

Word count: 3999, 6 figures

Graphical abstract

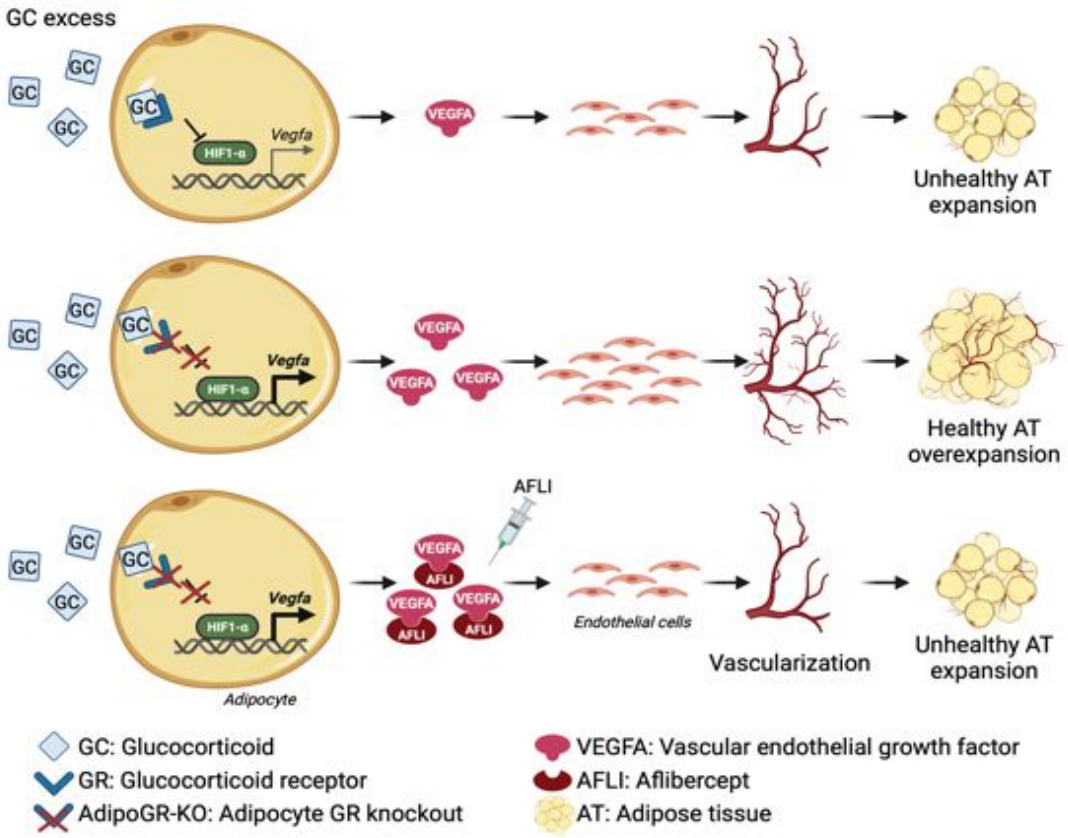

Figure created with BioRender.com

Abstract

Glucocorticoids (GC) are commonly prescribed because of their anti-inflammatory and immunosuppressive properties. However, high doses of GC often lead to adverse side effects including diabetes and lipodystrophy. We recently reported that adipocyte glucocorticoid receptor (GR)-deficient (AdipoGR-KO) mice under corticosterone (CORT) treatment exhibited a massive adipose tissue (AT) expansion associated with a paradoxical improvement of metabolic health compared to control mice. However, whether GR may control adipose development remains unclear. Here, we show a specific induction of the hypoxia-inducible factor HIF-1α and the pro-angiogenic Vascular Endothelial Growth Factor-A expression in GR-deficient adipocytes of AdipoGR-KO mice as compared to control mice, together with an increased adipose vascular network, as assessed by 3D-analysis imaging. GR activation reduced HIF-1α recruitment on *Vegfa* promoter resulting from *Hif-1α* down-regulation at the transcriptional and post-translational levels. Importantly, in CORT-treated AdipoGR-KO mice, the blockage of VEGFA by a soluble decoy receptor prevented AT expansion and the healthy metabolic phenotype. Finally, in subcutaneous AT from Cushing patients, higher VEGFA expression was associated with a better metabolic profile. Collectively, these results highlight that adipocyte GR negatively controls AT expansion and metabolic health through the down-regulation of the major angiogenic effector VEGFA and inhibiting vascular network development. (LIPOCUSH, NCT01688349)

Article Highlights

- Our previous study demonstrated that adipocyte glucocorticoid receptor (GR) deficiency protects mice from glucocorticoid (GC)-induced deleterious metabolic effects. Interestingly, this health improvement was associated with a massive expansion of their adipose tissue.

- Here we determined the role of GC/GR signaling on adipose tissue expansion and vascularization.

- GR suppresses adipose tissue vascularization by decreasing the vascular factor VEGFA and its transcriptional regulator HIF-1α. Blocking VEGFA abrogates beneficial impacts of GR deficiency in GC-exposed mice. Cushing' patients with higher *VEGFA* expression in AT exhibit a healthier metabolic profile.

- Selectively antagonizing adipocyte GR could prevent GC metabolic adverse effects.

Introduction

Glucocorticoids (GC) and their synthetic analogues are a potent treatment for inflammatory diseases and are therefore among the most prescribed drugs. Nowadays, 1-1.2 % of the general population may undergo systemic GC therapy for months or years (1). However, prolonged GC exposure, as observed in patients with Cushing's syndrome, may lead to metabolic adverse events, including insulin resistance, hyperglycemia, dyslipidemia and lipodystrophy (2-4), suggesting a role for GC signaling in metabolic syndrome.

GC have diverse effects on adipose tissue (AT) biology, ranging from adipocyte precursor differentiation to the regulation of metabolic and endocrine functions in mature adipocytes (2, 3). The biological effects of cortisol (in humans) and corticosterone (in rodents) are mediated by both the mineralocorticoid receptor and the glucocorticoid receptor (GR), the latter being prominently involved in the metabolic alterations induced by GC (5, 6). These data strengthen the interest for studying the impact of GR activation on AT biology and metabolism.

This past decade, independent studies have reported the effect of the constitutive adipocyte-specific GR invalidation in mice under high fat diet (7-12) leading to contrasting phenotypes. To overcome potential compensatory mechanisms resulting from constitutive GR deficiency during AT development in mice, we generated an inducible model of selective adipocyte GR invalidation (AdipoGR-KO) in adult mice. Glucose intolerance and insulin resistance usually induced by the GR natural ligand corticosterone (CORT) in control mice were markedly reduced in AdipoGR-KO mice compared to their littermate controls (13). This metabolic improvement was associated with reduced hepatic steatosis and improved lipid profile. Interestingly, these beneficial effects were associated with a massive expansion of subcutaneous (SCAT) and gonadal AT (GAT) (13). These results were also consistent with higher adiposity and insulin sensitivity observed in constitutive GR-deficient mice despite GC

treatment (12, 14). Thus, selective GR deletion within adipocytes alleviated some adverse GC effects by favoring a healthy expansion of adiposity in AdipoGR-KO mice.

AT is a highly active tissue, whose expanse is accompanied by the development of an appropriate vascular network, adapted to the tissue size and to nutritional challenges (15-17). Blood flow ensures metabolic and oxygen exchanges, and delivers hormones and growth factors involved in whole body metabolic homeostasis (15, 16, 18). The vascular system controls AT microenvironment, which influences preadipocyte differentiation, AT function and plasticity (18). Blood vessel growth and angiogenesis is partly promoted by mild hypoxia through induction of the transcription factor HIF-1α (*Hypoxia-Inducible Factor-1α*) (20), which acts with its partner HIF-1β on hypoxia response elements (HREs) present in the promoter of the gene coding for VEGFA (*Vascular Endothelial Growth Factor-A*), a key angiogenic factor (17, 19). During obesity, the rapid increase in fat mass exceeds the vascular network expansion capacities, triggering AT inflammation and insulin resistance, and contributing to systemic metabolic alterations (17, 19, 20). Adipose-specific VEGFA overexpression improves AT vascularization and protects mice from high fat diet deleterious effects, while suppressing VEGFA in AT reduces adipose vascular network, promotes inflammation and the development of a severe insulin resistance (21-23). Angiogenesis adaptation therefore seems to be an early and crucial process for healthy AT expansion.

The aim of the current study was to show that adipocyte GR activation could directly preclude AT vascular network adaptation and, in turn, modulate whole body metabolic homeostasis. By combining *in vivo* and *in vitro* approaches, we unveiled a new mechanism in which the adipocyte GC/GR signaling restrains AT vascularization through the regulation of the HIF-1α/VEGFA pathway, therefore participating to the deleterious metabolic effects of GC.

Research Design and Methods

Animals and treatments

AdipoGR-KO mice were generated as described in (13). Treatments (tamoxifen, corticosterone and Aflibercept (AFLI)), and tissue and blood collection were detailed in Online Supplemental Material.

Metabolic parameters' exploration and *in vivo* insulin stimulation

Insulin tolerance test (ITT) and insulin pulse experiments were performed as described in (13) on 5-hour fasted mice, injected intraperitoneally with 1 IU/kg and 1.5 IU/kg of human insulin (Actrapid Penfill; Novo Nordisk, Paris, France), respectively. Hepatic triglycerides (TG) were extracted and measured with a colorimetric diagnostic kit according to manufacturer's instructions (Triglycerides FS, DiaSys, Grabels, France).

Histo-morphological procedures

Paraffin-embedded liver and adipose tissue (AT) were cut in 5-µm-thick sections and stained with hematoxylin and eosin. For CD31 staining, NOVOLINK Polymer Detection Systems kit was used according to manufacturer's recommendations (Leica, Buffalo Grove, IL, USA) (Supplementary Table 1). CD31 intensity was determined on 5 to 10 fields of SCAT and GAT per section covering the entire tissue surface, at original magnification x10 (optical microscope IX83; Olympus, Rungis, France) using ImageJ software (http://rsbweb.nih.gov/ij/). Results are expressed as region of interest (ROI) per mg of AT.

Isolation of adipocyte and stromal vascular fractions

When indicated, adipocyte and stromal vascular fractions (SVF) were isolated from SCAT and GAT of treated control and AdipoGR-KO mice as previously described in (13).

Flow cytometry

Freshly isolated SVF were incubated with fluorescent-conjugated antibodies or their respective controls (Supplementary Table 1). Flow cytometry was performed with a CytoFLEX cytometer (Beckman Coulter, Villepinte, France) and data analysis was conducted by FlowJo software (Becton, Dickinson and Company, Franklin Lakes, USA).

Cell culture

3T3-F442A preadipocytes (24) were maintained and differentiated as mentioned in Online Supplemental Material. Mature adipocytes were treated with indicated dexamethasone (Dex, Sigma-Aldrich) concentrations, with or without 100 μM of RU-486 (Sigma-Aldrich), under normoxic (21% O_2, 5% CO_2, and 74% N_2), or hypoxic condition (1% O_2, 5% CO_2, and 94% N_2) for 16 hours.

RNA extraction and RT-qPCR analysis

Total RNA extraction from human and mice tissues and adipocyte / SVF fractions are detailed in Online Supplemental Material.

Protein extraction and analysis

Details are provided in the Online Supplemental Material.

Chromatin Immunoprecipitation (ChIP)

ChIP assays were performed on mature 3T3-F442A adipocytes treated with 100 nM dexamethasone under normoxic or hypoxic condition for 16 hours with the Acetyl-histone H4 immunoprecipitation (ChIP) assay kit according to manufacturer's instructions (Sigma-

Aldrich) as previously described in (25) and detailed in Online Supplemental Material (Supplementary Tables 1 and 2).

AT clearing and 3D-fluorescence imaging

DyLight 649 labeled Lycopersicon Eculentum (Tomato) lectin (Vector Labs, Peterborough, UK) was systemically administered to the mice *via* the retro-orbital sinus 5 minutes before the sacrifice (Supplementary Table 1). Detailed methodology is provided in Online Supplemental Material.

Patients with Cushing's syndrome

Patients were diagnosed with endogenous ACTH-independent Cushing's syndrome, caused by benign adrenal gland adenoma. Cushing's syndrome diagnosis was made according to at least one of the three following parameters: an increase in urinary free cortisol, altered plasma cortisol after a 1 mg dexamethasone suppression test (DST), or a high midnight plasma cortisol, associated with a low ACTH plasma level. Sample collection processing, morphometric and metabolic parameters are described in Online Supplemental Material (Supplementary Tables 3 and 4).

Statistical Analysis

All values were expressed as the means +/- SEM. The normality was tested by Shapiro-Wilk test. For comparisons of two groups, data were analyzed using Student's t-tests. For multiple groups comparisons, data were analyzed using one-way ANOVA followed by Bonferroni *post hoc* analyses when appropriate or Kruskall-Wallis test. Correlations between human gene expression data, clinical and anthropometric parameters were analyzed by calculating

Spearman's coefficient. Test analyses were performed using Prism software Prism 8 (GraphPad Software, La Jolla, CA, USA). A P value < 0.05 was considered statistically significant.

Data and Resource Availability

Data sets and resources are available upon request.

Results

Adipocyte-specific GR deficiency prevents CORT-inhibition of adipocyte *Vegfa* and *Hif-1α* expression and promotes a healthy adipose tissue expansion

To analyze GR role on angiogenesis during CORT-induced AT expansion, we measured *Vegfa* and *Hif-1α* mRNA expression in whole SCAT and GAT or alternatively in isolated adipocyte and stromal vascular fractions (SVF), collected from AdipoGR-KO and littermate control (Ctrl) mice treated with vehicle (VEH) or CORT for 4 weeks.

CORT treatment drastically decreased *Vegfa* and *Hif-1α* mRNA levels in whole SCAT and GAT of control mice, and in the corresponding adipocyte fractions (Fig. 1A and 1B). In agreement, VEGFA protein content was reduced by 40-45% in the SCAT and GAT of CORT-treated control mice (Fig. 1C). Strikingly, adipocyte GR deficiency almost completely prevented the CORT-related down-regulation in *Vegfa* and *Hif-1α* mRNA expression in AT, and more specifically in their adipocyte fractions (Fig. 1A-1B, and Supplementary Fig. 1A). Accordingly, VEGFA protein concentration was increased by 2- to 4.5-fold in AT of CORT-treated AdipoGR-KO mice, when compared to their control mice (Fig. 1C), without impacting VEGFA plasma concentration (Supplementary Fig. 1B). Furthermore, GR deficiency in AT did not affect *Vegfa* and *Hif-1α* mRNA expression in the liver and skeletal muscles in mice under VEH and CORT treatment (Supplementary Fig. 1C). Notably, the increased *Vegfa* mRNA and protein expression in CORT-treated AdipoGR-KO mice is consistent with their AT massive expansion and preserved insulin sensitivity compared to control mice (Fig. 1D and 1E).

Interestingly, when comparing SCAT and GAT weight gain to *Vegfa* and *Hif-1α* expression after only 4 days of CORT treatment in control and AdipoGR-KO mice, we found an elevated fat depot weights (Supplementary Fig. 2A), associated with higher expression of *Vegfa* and *Hif-1α* mRNA in fat depots of AdipoGR-KO mice compared to control mice (Supplementary Fig.

2B). Altogether, these data demonstrate a functional link between adipocyte GR signaling and an early angiogenesis and AT expansion.

The GR agonist dexamethasone exerts an inhibitory effect on *Vegfa* and *Hif-1α* expression in cultured adipocytes

To investigate the regulation of adipose *Vegfa* and *Hif-1α* mRNA expression by GC, we treated 3T3-F442A adipocytes with different doses of dexamethasone (Dex), alone or in association with the GR antagonist RU-486 (Fig. 2A). As expected, the expression of the GR target gene *Fkbp5* was strongly induced by Dex, in a dose-dependent manner, up to 20-fold at 100 nM, and conversely inhibited in the presence of RU-486 (Fig. 2A). Consistent with *in vivo* data, *Vegfa* and *Hif-1α* expression was reduced by 50 and 60 %, respectively, upon Dex 100 nM treatment. RU-486 totally prevented the inhibitory action of Dex treatment on both genes (Fig. 2A), supporting the fact that *Vegfa* and *Hif-1α* regulation depends on GR activation.

We exposed 3T3-F442A adipocytes under hypoxia, a condition stabilizing HIF-1α protein and tested whether Dex could affect *Vegfa* and *Hif-1α* expression in this permissive condition. As expected, hypoxia induced glucose transporter *Slc2a1* and *Vegfa* mRNA expression (Fig. 2B) (26, 27). In this context, Dex treatment markedly reduced hypoxic induction of *Slc2a1* and *Vegfa* mRNA (Fig. 2B). In agreement with the known post-translational regulation of HIF-1α protein, hypoxia alone had little impact on *Hif-1α* mRNA expression (Fig. 2B), but increased the overall protein level (Fig. 2C). Dex decreased both *Hif-1α* mRNA and protein expression, suggesting a transcriptional and post-transcriptional GR-mediated HIF-1α regulation (Fig. 2B and 2C). Chromatin immunoprecipitation (ChIP) assay showed that Dex treatment decreased hypoxia-induced HIF-1α recruitment onto the *Vegfa* promoter (Fig. 2D), suggesting a reduced HIF-1α transcriptional activity. These results indicate that under Dex stimulation, GR down-regulates *Vegfa* expression through a decrease in *Hif-1α* expression and activity.

AdipoGR-KO mice exhibit increased adipose tissue vascularization under CORT treatment

To explore whether changes in *Vegfa* mRNA and protein levels affected AT angiogenesis and vascular network in CORT-treated AdipoGR-KO mice, we first performed flow cytometry analysis of CD31+/CD45- endothelial cells from SCAT and GAT. In control mice, CORT treatment decreased endothelial cell number compared to VEH-treated mice (Fig. 3A), consistent with CORT-induced down-regulation of *Vegfa* expression (Fig. 1A). Strikingly, adipocyte GR deficiency completely prevented this decrease in GAT, leading to a 3-fold increase in endothelial cell number compared to CORT-treated control mice (Fig. 3A). Although not significative, we observed a trend towards a higher number of endothelial cells in the SCAT of CORT-treated AdipoGR-KO mice (Fig. 3A). These results were confirmed by immunohistochemistry showing an increased endothelial cell (CD31) labeling in AT of AdipoGR-KO mice compared to control mice (Fig. 3B). To assess whether these changes were associated with vascular network remodeling, we performed 3D fluorescence imaging of cleared SCAT and GAT vascular network from control and AdipoGR-KO mice (Fig. 3C-3E). We observed a higher vascular volume in AT of CORT-treated AdipoGR-KO compared to their control mice (Fig. 3D and Supplementary Movies 1-8), suggesting that the adipocyte GR restrains AT vascularization and growth.

VEGFA is a key factor of adipose tissue vascularization and expansion in AdipoGR-KO mice under CORT treatment

To determine the role of VEGFA in the CORT-induced AT expansion in AdipoGR-KO mice, we treated animals in the same time as CORT with Aflibercept (AFLI), that binds VEGFA and blocks its action (28).

AFLI efficiency on the VEGFA/VEGFR2 signaling was validated on the expression of the target gene *Esm1* (*Endothelial cell-specific molecule 1*) (29). *Esm1* was up-regulated in SCAT and GAT of CORT-treated AdipoGR-KO mice compared to control mice and was decreased, as expected, by AFLI (Fig. 4A).

We then explored the consequences of altered VEGFA signaling on endothelial cell number by flow cytometry. Blocking VEGFA action in CORT-treated AdipoGR-KO mice drastically reduced endothelial cell number in comparison with mice treated with CORT alone (Fig. 4B). Moreover, AFLI and CORT combined treatment attenuated the greater body weight gain, fat mass and AT expansion observed in AdipoGR-KO mice treated with CORT alone (Fig. 4C-4F). Of note, AFLI alone had no significant impact on body and AT weights, except a slight decrease in the GAT of CORT-treated control mice (Supplementary Fig. 3A-3C). Therefore, these findings demonstrate that the crosstalk between GR-deficient adipocytes and endothelial cells through VEGFA secretion is necessary for AT expansion in AdipoGR-KO mice.

AFLI treatment suppresses the protective effect of GR deficiency on CORT-induced insulin resistance

CORT-treated AdipoGR-KO mice were, as expected, more sensitive to insulin than CORT-treated control animals (Fig. 5A and 1F). However, AFLI- and CORT-treated AdipoGR-KO mice reached an insulin resistance level similar to CORT-exposed control mice (Fig. 5A). We performed insulin pulse experiments to investigate the effect of AFLI treatment on the activation of insulin signaling in SCAT, GAT, and in the liver and measured Akt phosphorylation (Fig. 5B-5E). Immunoblot analysis indicated that AdipoGR-KO mice treated with CORT were protected from CORT-induced insulin resistance in SCAT and GAT, but not in the liver compared to control mice (Fig. 5B-5E). Importantly, AFLI treatment drastically impaired insulin-induced Akt phosphorylation in GAT and to a lesser extend in SCAT, but not

in the liver of CORT-treated AdipoGR-KO mice (Fig. 5B-5D). Overall, our data support the concept that AdipoGR-KO mice are less protected from CORT-induced insulin resistance when treated with AFLI and show that VEGFA is a prerequisite for the healthy AT expansion which is required to sustain insulin sensitivity.

AFLI treatment suppresses the protective effect of GR deficiency on CORT-induced hepatic steatosis

We previously demonstrated that GR-deficient mice were protected from hepatic steatosis and had lower triacylglycerol (TG) concentrations in their liver despite CORT exposure (13). To investigate whether AFLI treatment could impact CORT-induced hepatic steatosis, we performed hematoxylin/eosin staining on liver sections. As expected, CORT treatment led to liver steatosis in control mice, which was strongly reduced in AdipoGR-KO mice (Fig. 5F). GR-deficient mice treated with combined AFLI and CORT treatment were no longer protected from liver steatosis (Fig. 5F). Accordingly, hepatic TG concentration was drastically reduced in the liver of CORT-treated AdipoGR-KO compared to control mice, an effect that was abrogated under AFLI treatment (Fig. 5G). Thus, adipocyte GR plays a key role in the regulation of healthy AT expansion and therefore the protection against hepatic steatosis in AdipoGR-KO mice under CORT treatment.

Higher VEGFA expression in SCAT is associated with a healthier metabolic profile in patients with Cushing's syndrome

We assessed the pathophysiological relevance of GC-regulated *VEGFA* expression in a cohort of 20 patients with hypercortisolic adenoma (LIPOCUSH cohort). Patients' clinical, metabolic and anthropometric parameters are depicted in Supplementary Tables 3 and 4.

We determined whether *VEGFA* expression was correlated with a healthier metabolic profile. As observed in Figure 6A and Supplementary Table 5, *VEGFA* expression was negatively correlated with BMI and HOMA-IR, and positively correlated with the percentage of fat mass in the upper and lower limbs. We then divided the LIPOCUSH cohort in two subgroups according to their low or high level of *VEGFA* expression in SCAT, based on the stratified median (Fig. 6B). Patients with the highest expression of *VEGFA* displayed lower levels of insulin resistance (assessed by HOMA-IR index) and of glycated hemoglobin, HbA1c (Supplementary Table 3). No further changes were observed regarding cortisol production, plasma TG and free-fatty acids between both groups. "Higher VEGFA" patients presented an increase in the percentage of fat mass in upper and lower limbs despite similar percentage of total and trunk fat mass compared with patients expressing the lowest *VEGFA* level (Supplementary Table 4). Thus, higher *VEGFA* expression in Cushing's patients was associated with an improved metabolic phenotype and enhanced expansion of AT in limbs, likely acting as a protective 'metabolic sink' through its increased capacity of lipid buffering (30, 31).

We further explored whether expression of key markers of GC signaling, adipocyte differentiation and function were correlated to *VEGFA* expression (Fig. 6 and Supplementary Table 5). *VEGFA* expression was positively correlated with *NR3C1* (human GR gene) and adipocyte marker-related genes, while negatively correlated with the expression of *HSD11B1* (*11-beta hydroxysteroid dehydrogenase 1*), an enzyme responsible for local production of cortisol. The stratified analysis highlighted that higher *VEGFA* patients displayed an increased *NR3C1* expression while *HSD11B1* mRNA level was decreased (Fig. 6C). Furthermore, mRNA expression of early (*CCAAT-enhancer-binding protein C/EBPB, C/EBPD*) and late (*peroxisome proliferator–activated receptor γ PPARG, C/EBPA*) adipogenic transcription factors (Fig. 6D-6E), as well as lipogenic markers (*SREBF1* and *fatty acid synthase FASN*) (Fig. 6F) were also significantly increased in patients with the highest *VEGFA* expression, supporting

an improved adipocyte differentiation and lipid storage capacities. Finally, according to the decreased insulin resistance observed in high *VEGFA* patients, *ADIPOQ*, but not *LEP* mRNA expression was elevated (Fig. 6G). Collectively, these data show that hypercortisolic patients with lower level of *VEGFA* expression in SCAT exhibited a worsened metabolic profile as compared to patients with higher *VEGFA* expression, highlighting a combined action of VEGFA factor and GC/GR pathway in Human AT and metabolic homeostasis.

Discussion

We previously demonstrated that the selective deletion of the GR in AT counteracts several deleterious GC-induced metabolic effects leading to insulin resistance and diabetes (13). This improvement was associated with a massive expansion of AT in mice, suggesting a detrimental role of the GR in the healthy AT adaptation, an effect still poorly documented. In this study, we demonstrate for the first time that adipocyte GR acts as a central player of adipose vascular flexibility by repressing *Vegfa* expression and down-regulating VEGFA protein known as a cornerstone of AT plasticity (17). Supporting our hypothesis, Hayashi *et al* published a transcriptomic analysis showing that VEGF pathway was altered in AT of patients with a Cushing's syndrome (14). Hence, our main conclusion is that the adipocyte GC/GR signaling pathway negatively regulates AT vascularization, thereby precluding healthy AT expansion and whole-body metabolic homeostasis.

AT exhibits remarkable plasticity and expansion capacities, requiring the development of new vessels to support an adequate supply of oxygen and nutrients (15, 32, 33). However, an altered synergy between AT expansion and vascularization, as observed during obesity, may lead to hypoxia, inflammation and impaired AT function (19, 34). VEGFA is crucial to regulate this process as previously documented by others (21-23). In the present study, CORT treatment in control mice led to metabolic deleterious effects, which coincides with decreased *Vegfa* expression in AT. This effect was counteracted by the absence of adipocyte GR, suggesting a GC- and GR-dependent *Vegfa* expression. Surprisingly, despite a strong induction of VEGFA in AT, plasma levels remained stable in AdipoGR-KO mice, indicating a paracrine, rather than an endocrine effect of adipocyte VEGFA on endothelial cells to promote vascular network and AT expansion. These results are consistent with the work of Elias *et al* (23), showing that adipocyte *Vegfa* overexpression had no impact on VEGFA plasma levels. Moreover, our data

are also in line with the increased adipocyte *Vegfa* expression observed in total HSD11B1-deficient obese mice (35, 36). Nevertheless, due to our unique inducible adipose-specific mouse model, we are the first to show that adipocyte GR signaling exerts a significant role on AT vascular adaptation and plasticity through VEGFA, therefore controlling whole-body insulin sensitivity.

A link between GR signaling and VEGFA suppression has been suggested in adipose and non-adipose tissues (37, 38), however the molecular mechanism still remains elusive. We raised several hypotheses to explain *Vegfa* modulation by GC/GR signaling. No Glucocorticoid Responsive Elements (GRE) consensus site has been reported on *Vegfa* promoter (39). Therefore, HIF-1α, one of the major transcription regulators of *VEGFA*, appears as a relevant molecular mediator of GC action. Deletion of adipocyte *Phd2* (Prolyl-hydroxylase domain protein 2) in mice results in stabilization of HIF proteins leading to a pseudo-hypoxia condition, and an increased adiposity associated with a beneficial AT vascularization (40). Similarly, we showed a significant induction of *Hif-1α*, closely related to *Vegfa* expression, in adipose depots of CORT-treated AdipoGR-KO mice. Experiments on mature 3T3-F442A adipocytes showed a concomitant regulation of the *Vegfa* and *Hif-1α* contents by Dex, involving transcriptional and post-translational HIF-1α changes and a reduced binding on *Vegfa* promoter. Collectively, these *in vivo* and *in vitro* approaches indicate that GR signaling decreases HIF-1α activity on *Vegfa* promoter, leading to a reduced *Vegfa* expression. However, the absence of GRE consensus sites in *Hif-1α* promoter suggests a more complex level of regulation by GC/GR pathway (41).

Our thorough study supports the fact that the improved metabolic profile in AdipoGR-KO mice was partly due to an enhanced SCAT and GAT vascularization. While CORT decreased the

number of CD31 endothelial cells in AT of control mice, adipocyte GR deletion prevented CORT-induced endothelial cell decline. Through the innovative technique of whole AT clearing coupled to 3D volume fluorescence-imaging (18, 42, 43), we showed that these data were associated with a higher density of adipose vascular network, characterized by an increased vessel volume rather than a change in their length in AT of AdipoGR-KO mice. The overall higher density of capillaries may favor the interaction surface with the surrounding adipocytes and therefore contributes to adipocyte lipid storage and expansion.

To determine the contribution of VEGFA in the healthy AT expansion of AdipoGR-KO mice, we used AFLI combined with either VEH or CORT treatment to block VEGFA action. AFLI is used in human colorectal cancer or diabetic retinopathy (28, 44, 45). This recombinant protein was engineered by the fusion of two extracellular domains of VEGF receptor 1 and 2 to the heavy chain portion of human immunoglobulin G1. AFLI prevents VEGFA, VEGFB and to a lower affinity PIGF binding to their receptors on endothelial cells. Blocking VEGFA action on endothelial cells impedes AT growth and development, and results in the loss of beneficial effects of GR deficiency on insulin resistance and liver steatosis. Altogether, our study highlights the major role of VEGFA in the healthy expansion of AT in mice with deleted adipocyte GR.

Finally, we assessed the relevance of our findings in a cohort of Cushing's syndrome patients due to adrenal cortisolic adenoma. Patients with the highest *VEGFA* expression showed an improved glycemic profile associated to an increased expression of the insulin-sensitizing adipokine, adiponectin. These patients also exhibited a higher expression of the main markers of adipocyte differentiation and lipogenesis in SCAT, suggesting a healthy and insulin sensitive AT. Although our human study has some limitations due to the small number of selected

patients, these data strengthen our *in vitro* and *in vivo* conclusions in mice, regarding the role of VEGFA and angiogenesis in the control of AT expansion and metabolic homeostasis under hypercorticism.

In conclusion, this new facet of adipocyte GR action on the physiology and pathophysiology of AT will help to define future therapeutic strategies aiming at reducing deleterious metabolic effects of GC. Research to date has focused on developing selective GR modulators (SGRMs) that retain the anti-inflammatory properties of GC, but limit their metabolic or bone side effects (46, 47). However, due the complexity of GR signaling regulation at the molecular level, and based on our results, it seems relevant to consider innovative approaches to selectively antagonize the GR specifically in adipocytes, to prevent GC metabolic adverse effects such as insulin resistance and hepatic steatosis.

Acknowledgments. The authors are grateful to Dr B. Gaugler (INSERM, Saint-Antoine Research Center, Sorbonne University, Paris) for her helpful assistance on flux cytometry, and M. Auclair, A. Mevel, D. Moret (all from INSERM, Saint-Antoine Research Center, Sorbonne University, Paris) for their technical assistance. The authors thank L. Dinard, A. Guyomard, T. Coulais, and Q. Pointout (Animal housing facility), B. Solhonne (Histomorphology Platform), R. Morrichon (Cell Imaging and Confocal Microscopy Platform), and A. Munier (Cytometry Platform) of the Saint-Antoine Research Center (Sorbonne University, INSERM, Paris) for their excellent support. We thank A. Larsen, M. Sabbah (Saint-Antoine Research Center, Sorbonne University, INSERM, Paris) and E. Girault (Assistance Publique des Hôpitaux de Paris, Hôpital Saint-Antoine, Paris, France) for providing Aflibercept and L. Louadj (Saint-Antoine Research Center, Sorbonne University, INSERM, Paris) for helping with cultures under hypoxic condition. We thank the patients who participated to the LIPOCUSH Study and LIPOCUSH investigators (Pr P. Chanson, Pr P. Kamenicky, Dr E. Khun, Dr B. Parier from Bicêtre Hospital, Le Kremlin Bicêtre, France; Pr J. Bertherat, Dr L. Bricaire, Dr L. Guignat from Cochin Hospital, Paris, France; Dr C. Ajzenberg, From Mondor Hospital, Créteil, France; Dr S. Gaujoux, Pr F. Menegaux, Dr C. Jublanc, from Pitié Salpêtrière Hospital, Paris, France; Pr A. Tabarin, from Haut-Lévêque Hospital, Bordeaux, France; Pr S.Christin-Maitre from Saint-Antoine Hospital, Paris, France; Pr P. Sebe From Tenon Hospital and Diaconèses Hospital, Paris, France). The authors warmly thank K.E. Davis (UT Southwestern Medical Center, USA) for helpful reading and discussion.

Funding. This work was supported by grants from INSERM, Sorbonne University, French Society of Diabetes (Société Francophone pour le Diabète [SFD] Allocation number: RAK18021DDA) and the Medical Research Foundation (Fondation pour la Recherche Médicale [FRM] EQU201903007868). A.V. and H.D. were both supported by doctoral

fellowship from Ministère de l'Enseignement Supérieur et de la Recherche and an additional one-year grant from FRM for H.D.

Duality of interests. The authors have declared that no conflict of interest exists regarding the present study.

Author contributions. AV, HD and MG performed and analyzed gene expression and protein experiments in culture and conditional knockout mice. AV, HD, AG, BB, CB, NR, MG, TL and MM performed treatment, metabolic exploration and biochemical analysis of conditional knockout mice. AV and KP performed and analyzed flux cytometry experiments; EH performed ChIP studies on cultured adipocytes; NR, AV and MG performed and analyzed adipose tissue and liver histology; TL performed animal injection of fluorescent (Tomato) lectin, and JG achieved adipose tissue clearing and analyses for AT clearing. CV and BF recruited patients for the LIPOCUSH cohort. AV, CD, CV, JC and BF performed and analyzed studies on LIPOCUSH cohort of patients. AV, HD, JC, MC, JFT, JG, AG, BF and MM contributed to manuscript preparation, writing, analysis of the data, generation of all figures, data discussion and manuscript editing.

References

1. Fardet L, Fève B. Systemic glucocorticoid therapy: a review of its metabolic and cardiovascular adverse events. Drugs. 2014;74: 1731-1745
2. Lee M, Pramyothin P, Karastergiou K, Fried S. Deconstructing the roles of glucocorticoids in adipose tissue biology and the development of central obesity. Biochim Biophys Acta. 2014;1842: 473-481
3. Ferraù F, Korbonits M. Metabolic comorbidities in Cushing's syndrome. Eur J Endocrinol. 2015;173: M133-157
4. Radhakutty A, Burt M. Management of endocrine disease : Critical review of the evidence underlying management of glucocorticoid-induced hyperglycaemia. Eur J Endocrinol. 2018;179: R207-R218
5. Fleseriu M, Biller B, Findling J, Molitch M, Schteingart D, Gross C, Investigators SS. Mifepristone, a glucocorticoid receptor antagonist, produces clinical and metabolic benefits in patients with Cushing's syndrome. J Clin Endocrinol Metab. 2012;97: 2039-1049
6. Wallia A, Colleran K, Purnell J, Gross C, Molitch M. Improvement in insulin sensitivity during mifepristone treatment of Cushing syndrome: early and late effects. Diabetes Care. 2013;36: e147-148
7. Abulizi A, Camporez J, Jurczak M, Høyer K, Zhang D, Cline G, Samuel V, Shulman G, Vatner D. Adipose glucocorticoid action influences whole-body metabolism via modulation of hepatic insulin action. FASEB J 2019;33: 8174-8185
8. Bose SK, Hutson I, Harris CA. Hepatic Glucocorticoid Receptor Plays a Greater Role Than Adipose GR in Metabolic Syndrome Despite Renal Compensation. Endocrinology 2016;157: 4943-4960
9. De Kloet AD, Krause EG, Solomon MB, Flak JN, Scott KA, Kim DH, Myers B, Ulrich-Lai YM, Woods SC, Seeley RJ, Herman JP. Adipocyte glucocorticoid receptors mediate fat-to-brain signaling. Psychoneuroendocrinology 2015;56: 110-119
10. Desarzens S, Faresse N. Adipocyte glucocorticoid receptor has a minor contribution in adipose tissue growth. J Endocrinol 2016;230: 1-11
11. Mueller KM, Hartmann K, Kaltenecker D, Vettorazzi S, Bauer M, Mauser L, Amann S, Jall S, Fischer K, Esterbauer H, Muller TD, Tschop MH, Magnes C, Haybaeck J, Scherer T, Bordag N, Tuckermann JP, Moriggl R. Adipocyte Glucocorticoid Receptor Deficiency Attenuates Aging- and HFD-Induced Obesity and Impairs the Feeding-Fasting Transition. Diabetes 2017;66: 272-286
12. Shen Y, Roh HC, Kumari M, Rosen ED. Adipocyte glucocorticoid receptor is important in lipolysis and insulin resistance due to exogenous steroids, but not insulin resistance caused by high fat feeding. Mol Metab 2017;6: 1150-1160
13. Dalle H, Garcia M, Antoine B, Boehm V, Do T, Buyse M, Ledent T, Lamazière A, Magnan C, Postic C, Denis R, Luquet S, Fève B, Moldes M. Adipocyte Glucocorticoid Receptor Deficiency Promotes Adipose Tissue Expandability and Improves the Metabolic Profile Under Corticosterone Exposure. Diabetes. 2019;68: 305-317
14. Hayashi R, Okuno Y, Mukai K, Kitamura T, Hayakawa T, Onodera T, Murata M, Fukuhara A, Imamura R, Miyagawa Y, Nonomura N, Otsuki M, Shimomura I. Adipocyte GR Inhibits Healthy Adipose Expansion Through Multiple Mechanisms in Cushing Syndrome. Endocrinology 2019;160: 504-521
15. Cao Y. Angiogenesis modulates adipogenesis and obesity. J Clin Invest. 2007;117: 2362-2368
16. Corvera S, Gealekman O. Adipose tissue angiogenesis: impact on obesity and type-2 diabetes. Biochim Biophys Acta. 2014;1842: 463-472

17. Herold J, Kalucka J. Angiogenesis in Adipose Tissue: The Interplay Between Adipose and Endothelial Cells. Front Physiol. 2021;11: 624903
18. Cao Y. Angiogenesis and vascular functions in modulation of obesity, adipose metabolism, and insulin sensitivity. Cell Metab 2013;18: 478-489
19. Trayhurn P. Hypoxia and adipocyte physiology: implications for adipose tissue dysfunction in obesity. Annu Rev Nutr. 2014;34: 207-236
20. Ye J, Gao Z, Yin J, He Q. Hypoxia is a potential risk factor for chronic inflammation and adiponectin reduction in adipose tissue of ob/ob and dietary obese mice. Am J Physiol Endocrinol Metab. 2007;293: E1118-1128
21. Sung H, Doh K, Son J, Park J, Bae Y, Choi S, Nelson S, Cowling R, Nagy K, Michael L, Koh G, Adamson S, Pawson T, Nagy A. Adipose vascular endothelial growth factor regulates metabolic homeostasis through angiogenesis. Cell Metab. 2013;17: 61-72
22. Sun K, Wernstedt Asterholm I, Kusminski C, Bueno A, Wang Z, Pollard J, Brekken R, Scherer P. Dichotomous effects of VEGF-A on adipose tissue dysfunction. Proc Natl Acad Sci U S A. 2012;109: 5874-5879
23. Elias I, Franckhauser S, Ferre T, Vila L, Tafuro S, Munoz S, Roca C, Ramos D, Pujol A, Riu E, Ruberte J, Bosch F. Adipose tissue overexpression of vascular endothelial growth factor protects against diet-induced obesity and insulin resistance. Diabetes 2012;61: 1801-1813
24. Green H, Kehinde O. Spontaneous heritable changes leading to increased adipose conversion in 3T3 cells. Cell. 1976;7: 105-113
25. Milet C, Bléher M, Allbright K, Orgeur M, Coulpier F, Duprez D, Havis E. Egr1 deficiency induces browning of inguinal subcutaneous white adipose tissue in mice. Sci Rep. 2017;7: 16153
26. Ebert B, Firth J, Ratcliffe P. Hypoxia and mitochondrial inhibitors regulate expression of glucose transporter-1 via distinct Cis-acting sequences. J Biol Chem. 1995;270: 29083-29089
27. Lolmède K, Durand De Saint Front V, Galitzky J, Lafontan M, Bouloumié A. Effects of hypoxia on the expression of proangiogenic factors in differentiated 3T3-F442A adipocytes Int J Obes Relat Metab Disord. 2003;27: 1187-1195
28. Holash J, Davis S, Papadopoulos N, Croll S, Ho L, Russell M, Boland P, Leidich R, Hylton D, Burova E, Ioffe E, Huang T, Radziejewski C, Bailey K, Fandl J, Daly T, Wiegand S, Yancopoulos G, Rudge J. VEGF-Trap: A VEGF blocker with potent antitumor effects. PNAS 2002;99: 11393-11398
29. Rocha S, Schille M, Jing D, Li H, Stefan Butz S, Vestweber D, Biljes D, Drexler H, Nieminen-Kelhä M, Vajkoczy P, Adams S, Benedito R, Adams R. Esm1 modulates endothelial tip cell behavior and vascular permeability by enhancing VEGF bioavailability. Circ Res. 2014;115: 581-590
30. Jung S, Park J, Seo Y. Relationship between arm-to-leg and limbs-to-trunk body composition ratio and cardiovascular disease risk factors. Sci Rep. 2021;11: 17414
31. Snijder M, Dekker J, Visser M, Bouter L, Stehouwer C, Yudkin J, Heine R, Nijpels G, Seidell J, Study H. Trunk fat and leg fat have independent and opposite associations with fasting and postload glucose levels: the Hoorn study. Diabetes Care. 2004;27: 372-377
32. Rupnick M, Panigrahy D, Zhang C, Dallabrida S, Lowell B, Langer R, Folkman M. Adipose tissue mass can be regulated through the vasculature. Proc Natl Acad Sci U S A. 2002;99: 10730-10735
33. Nishimura S, Manabe I, Nagasaki M, Hosoya Y, Yamashita H, Fujita H, Ohsugi M, Tobe K, Kadowaki T, Nagai R, Sugiura S. Adipogenesis in obesity requires close interplay between differentiating adipocytes, stromal cells, and blood vessels. Diabetes. 2007;56: 1517-1526

34. Hosogai N, Fukuhara A, Oshima K, Miyata Y, Tanaka S, Segawa K, Furukawa S, Tochino Y, Komuro R, Matsuda M, Shimomura I. Adipose tissue hypoxia in obesity and its impact on adipocytokine dysregulation. Diabetes 2007;56: 901-911
35. Small G, Hadoke P, Sharif I, Dover A, Armour D, Kenyon C, Gray G, Walker B. Preventing local regeneration of glucocorticoids by 11beta-hydroxysteroid dehydrogenase type 1 enhances angiogenesis. Proc Natl Acad Sci U S A. 2005;102: 12165-12170
36. Michailidou Z, Turban S, Miller E, Zou X, Schrader J, Ratcliffe P, Hadoke P, Walker B, Iredale J, Morton N, Seckl J. Increased angiogenesis protects against adipose hypoxia and fibrosis in metabolic disease-resistant 11β-hydroxysteroid dehydrogenase type 1 (HSD1)-deficient mice. J Biol Chem. 2012;287: 4188-4197
37. Greenberger S, Boscolo E, Adini I, Mulliken J, Bischoff J. Corticosteroid suppression of VEGF-A in infantile hemangioma-derived stem cells. N Engl J Med 2010;362: 1005-1013
38. Nauck M, Karakiulakis G, Perruchoud A, Papakonstantinou E, Roth M. Corticosteroids inhibit the expression of the vascular endothelial growth factor gene in human vascular smooth muscle cells. Eur J Pharmacol 1998;341: 309-315
39. Pagès G, Pouysségur J. Transcriptional regulation of the Vascular Endothelial Growth Factor gene-a concert of activating factors. Cardiovasc Res. 2005;65: 564-573
40. Michailidou Z, Morton N, Moreno Navarrete J, West C, Stewart K, Fernández-Real J, Schofield C, Seckl J, Ratcliffe P. Adipocyte pseudohypoxia suppresses lipolysis and facilitates benign adipose tissue expansion. Diabetes. 2015;64: 733-745
41. Minet E, Ernest I, Michel G, Roland I, Remacle J, Raes M, Michiels C. HIF1A gene transcription is dependent on a core promoter sequence encompassing activating and inhibiting sequences located upstream from the transcription initiation site and cis elements located within the 5'UTR. Biochem Biophys Res Commun. 1999;261: 534-540
42. Barreau C, Labit E, Guissard C, Rouquette J, Boizeau M, Gani Koumassi S, Carrière A, Jeanson Y, Berger-Müller S, Dromard C, Plouraboué F, Casteilla L, Lorsignol A. Regionalization of browning revealed by whole subcutaneous adipose tissue imaging. Obesity (Silver Spring). 2016;24: 1081-1089
43. Chi J, Wu Z, Choi C, Nguyen L, Tegegne S, Ackerman S, Crane A, Marchildon F, Tessier-Lavigne M, Cohen P. Three-Dimensional Adipose Tissue Imaging Reveals Regional Variation in Beige Fat Biogenesis and PRDM16-Dependent Sympathetic Neurite Density. Cell Metab. 2018;27: 226-236
44. Syed Y, Mckeage K. Aflibercept: A Review in Metastatic Colorectal Cancer. Drugs 2015;75: 1435-1445
45. Anguita R, Tasiopoulou A, Shahid S, Roth J, Sim S, Patel P. A Review of Aflibercept Treatment for Macular Disease. Ophthalmol Ther. 2021;10: 413-428
46. Vandewalle J, Luypaert A, De Bosscher K, Libert C. Therapeutic Mechanisms of Glucocorticoids. Trends Endocrinol Metab. 2018;29: 42-54
47. De Nicola A, Meyer M, Guennoun R, Schumacher M, Hunt H, Belanoff J, De Kloet E, Gonzalez Deniselle M. Insights into the Therapeutic Potential of Glucocorticoid Receptor Modulators for Neurodegenerative Diseases. Int J Mol Sci. 2020;21: 2137

Figure titles and legends

Figure 1. Adipocyte-specific *Gr* deficiency prevents CORT-down-regulation of adipose *Vegfa* and *Hif-1α* expression and promotes a healthy adipose tissue expansion

Control (Ctrl) and AdipoGR-KO mice were exposed to VEH or corticosterone (CORT) during 4 weeks. *A, B*: Relative gene expression of *Vegfa* and *Hif-1α* was determined by RT-qPCR (*A*) in total subcutaneous (SCAT) and gonadal adipose tissue (GAT) extracts (n = 10-12/group) and (*B*) in the adipocyte fraction (n = 8-14/group). *C*: VEGFA protein concentration was measured in total extracts of SCAT and GAT of VEH- and CORT-treated Ctrl and AdipoGR-KO mice (n = 5-6/group). *D*: Weight of SCAT and GAT was reported as a percent of body weight for each mouse (n = 10-12/group). *E*: Insulin tolerance test (ITT) was performed on mice fasted for 5 hours before insulin intraperitoneal injection (1 IU/kg) (n = 10-11/group). Glucose levels were determined at indicated times (left panel) and areas of the curve were determined (AOC, right panel) for each ITT.

Data are presented as the mean +/- SEM. Each data point represents one animal. **P*<0.05, ***P*<0.01 and ****P*<0.001, as determined by Kruskal-Wallis test and one-way ANOVA, followed by the Bonferroni post-hoc test to compare means.

See also Supplementary Fig. 1 and 2.

Figure 2. The GR agonist dexamethasone inhibits *Vegfa* and *Hif-1α* expression in 3T3-F442A mature adipocytes

3T3-F442A mature adipocytes were treated with the indicated concentrations of the selective-GR agonist dexamethasone (Dex) in the presence or absence of the antagonist RU-486 (RU) during 16 hours. *A*: Relative gene expression of *Fkbp5, Vegfa* and *Hif-1α* was determined in response to different doses of Dex, with or without 100 μM RU-486 (n = 3-8 experiments).

B-D: 3T3-F442A mature adipocytes were placed under normoxic or hypoxic condition, in the presence or absence of 100 nM Dex during 16 hours. (*B*) *Slc2a1, Vegfa* and *Hif-1α* relative gene expression was measured by RT-qPCR (n = 4 experiments). (*C*) Representative Western blot and quantification of HIF-1α protein (n = 6 experiments). (*D*) ChIP analysis of HIF-1α binding onto *Vegfa* promoter. Immunoprecipitation (IP) was conducted with HIF-1α antibody. The DNA region of the *Vegfa* promoter was amplified by qPCR (n = 3 experiments).

Data are presented as the mean +/- SEM. Each data point represents one experiment performed in triplicate except in panel D where each data point represents one experiment. **P*<0.05, ***P*<0.01 and ****P*<0.001, as determined by Kruskal-Wallis test and one-way ANOVA, followed by the Bonferroni post-hoc test to compare means.

Figure 3. AdipoGR-KO mice exhibit an increased AT vascularization under CORT treatment

Control (Ctrl) and AdipoGR-KO mice were analyzed after a 4-week exposure to VEH or CORT. *A*: Flow cytometry analysis of endothelial cells was performed on the stromal vascular fraction (SVF) isolated from subcutaneous adipose tissue (SCAT) and gonadal adipose tissue (GAT) of VEH- and CORT-treated animals. Number of CD31+/CD45- endothelial cells in SCAT and GAT was determined per mg of AT (n = 6-16/group). *B*: Representative pictures of CD31 labeling (pointed by arrows, left panel) on SCAT and GAT sections from CORT-treated Ctrl and AdipoGR-KO mice and quantification (right panel) of CD31 intensity (ROI) per adipocyte (n = 4-8/group). *C*: Representative perspective 3D projection image of the vasculature in SCAT and GAT of treated mice. Fluorescent (Tomato) lectin was used as a marker of blood vessels in cleared AT. *D*: Quantification of vasculature as percent of vessel volume per AT volume (n = 2-3/group).

Data are presented as the mean +/- SEM. Each data point represents one animal. *P<0.05 and **P<0.01, as determined by a student's t test, Kruskal-Wallis test and one-way ANOVA, followed by the Bonferroni post-hoc test to compare means.

Figure 4. Aflibercept prevents adipose tissue angiogenesis and expansion in CORT-treated AdipoGR-KO mice

Control (Ctrl) and AdipoGR-KO mice were treated with CORT alone or in combination with the soluble decoy receptor, Aflibercept (AFLI) or the diluent (PBS) during 4 weeks. *A*: Relative gene expression of *Esm1* was determined by RT-qPCR in subcutaneous adipose tissue (SCAT) and gonadal adipose tissue (GAT) of Ctrl and AdipoGR-KO mice (n = 10-12/group). *B*: Flow cytometry analysis of endothelial cells was performed on the stromal vascular fraction (SVF) isolated from SCAT and GAT of CORT-treated mice. Number of CD31+/CD45- endothelial cells in SCAT and GAT was determined per mg of AT (n = 6-16/group). Of note, flow cytometry on AFLI groups were performed simultaneously with the groups presented in Fig. 3A. *C*: Body weight gain is presented after 4 weeks of treatment (n = 12-18/group). *D*: Fat body composition was determined by DEXA analyzer (n = 6-12/group). *E-F*: Subcutaneous adipose tissue (SCAT) and gonadal adipose tissue (GAT) weights are presented as the percentage of total body weight of Ctrl and AdipoGR-KO mice (n = 13-16/group).

Data are presented as the mean +/- SEM. Each data point represents one animal. *P<0.05, **P<0.01 and ***P<0.001, as determined by Kruskal-Wallis test and one-way ANOVA, followed by the Bonferroni post-hoc test to compare means.

See also Supplementary Fig. 2.

Figure 5. Blocking VEGFA impairs insulin sensitivity in CORT-treated AdipoGR-KO mice

Control (Ctrl) and AdipoGR-KO mice were treated with CORT in combination with the soluble decoy receptor, Aflibercept (AFLI) or its diluent (PBS) during 4 weeks. *A*: Insulin tolerance test (ITT) was performed on Ctrl and AdipoGR-KO mice fasted for 5 h (n = 10-20/group). Glucose levels were determined at indicated times (left panel) and the area of the curve was determined (AOC, right panel) for each ITT. *B-E*: Insulin pulses were performed in Ctrl and AdipoGR-KO mice. Quantification of insulin-stimulated phosphorylation of (P-)Akt to total Akt in (*B*) subcutaneous adipose tissue (SCAT), (*C*) gonadal adipose tissue (GAT), and (*D*) liver (n = 3-6/group). (*E*) Representative cropped Western blots are presented. *F*: Representative hematoxylin and eosin staining of liver sections of Ctrl and AdipoGR-KO mice. *G*: Liver triglyceride (TG) content were analyzed (n = 8-10/group).

Data are presented as the mean +/- SEM. **P*<0.05, and ****P*<0.001, as determined by Kruskal-Wallis test and one-way ANOVA, followed by the Bonferroni post-hoc test to compare means.

Figure 6. Higher human *VEGFA* expression in SCAT is associated with healthier metabolic profile

(*A*) Spearman correlation heatmap indicates correlation between *VEGFA* expression in the SCAT of patients with Cushing's syndrome (LIPOCUSH cohort) and their clinical, anthropometric and molecular traits. Intensities of blue and red colors indicate values of positive and negative correlation coefficients, respectively Rho correlations and *P* values are detailed in the figure and in the Supplementary Table 5. **P*<0.05, ***P*<0.01 and ****P*<0.001. (*B-G*) Twenty patients with Cushing's syndrome were divided into two subgroups according to their lowest and highest levels of *VEGFA* expression in SCAT, based on the stratified median of *VEGFA* gene expression. The two subgroups (low and high *VEGFA* expression) were compared to each other in term of gene expression of (*B*) *VEGFA*, (*C*) *NR3C1* and *HSD11B1*, (*D*) early (*C/EBPB, C/EBPD*), and (*E*) late (*C/EBPA* and *PPARG*) adipogenic transcription

factors, (*F*) lipogenic markers (*SREBF1* and *FASN*) and (*G*) adipokines (*LEP* and *ADIPOQ*), (n = 10 patients/group).

Each data point represents one patient. Data are presented as the mean +/- SEM. **P*<0.05, ***P*<0.01 and ****P*<0.001, as determined by Student's *t* Welch and Mann-Whitney test to compare means.

See also Supplementary Tables 3 and 4.

Figure 1

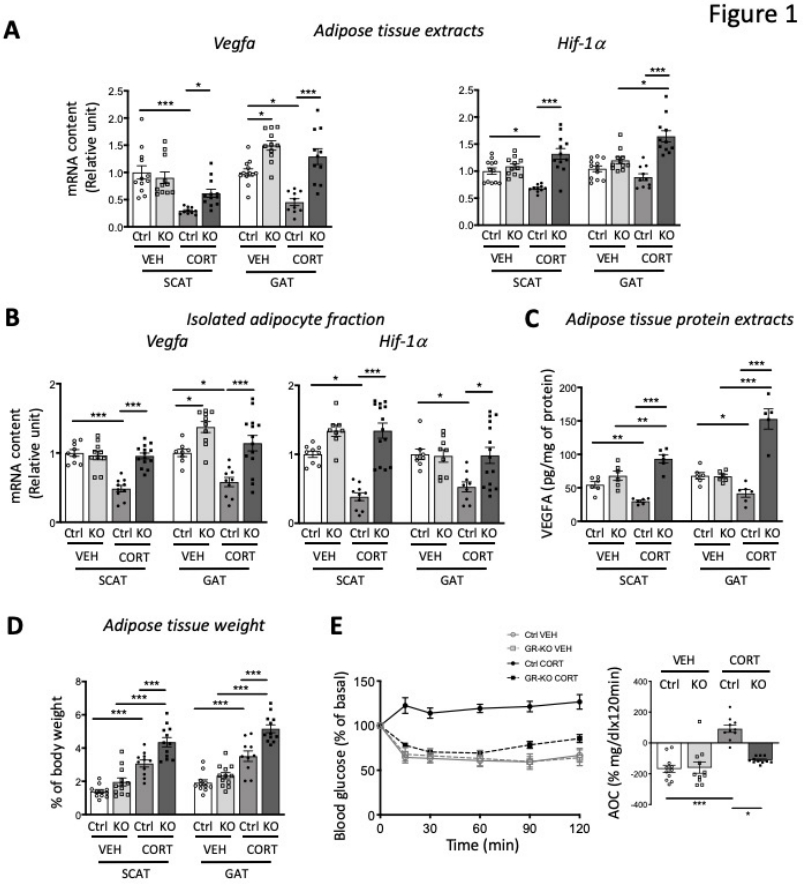

Figure 1. Adipocyte-specific Gr deficiency prevents CORT-down-regulation of adipose Vegfa and Hif-1α expression and promotes a healthy adipose tissue expansion

Control (Ctrl) and AdipoGR-KO mice were exposed to VEH or corticosterone (CORT) during 4 weeks. A, B: Relative gene expression of Vegfa and Hif-1α was determined by RT-qPCR (A) in total subcutaneous (SCAT) and gonadal adipose tissue (GAT) extracts (n = 10-12/group) and (B) in the adipocyte fraction (n = 8-14/group). C: VEGFA protein concentration was measured in total extracts of SCAT and GAT of VEH- and CORT-treated Ctrl and AdipoGR-KO mice (n = 5-6/group). D: Weight of SCAT and GAT was reported as a percent of body weight for each mouse (n = 10-12/group). E: Insulin tolerance test (ITT) was performed on mice fasted for 5 hours before insulin intraperitoneal injection (1 IU/kg) (n = 10-11/group). Glucose levels were determined at indicated times (left panel) and areas of the curve were determined (AOC, right panel) for each ITT.

Data are presented as the mean +/- SEM. Each data point represents one animal. *P<0.05, **P<0.01 and ***P<0.001, as determined by Kruskal-Wallis test and one-way ANOVA, followed by the Bonferroni post-hoc test to compare means.

See also Supplementary Fig. 1 and 2.

190x275mm (96 x 96 DPI)

Figure 2

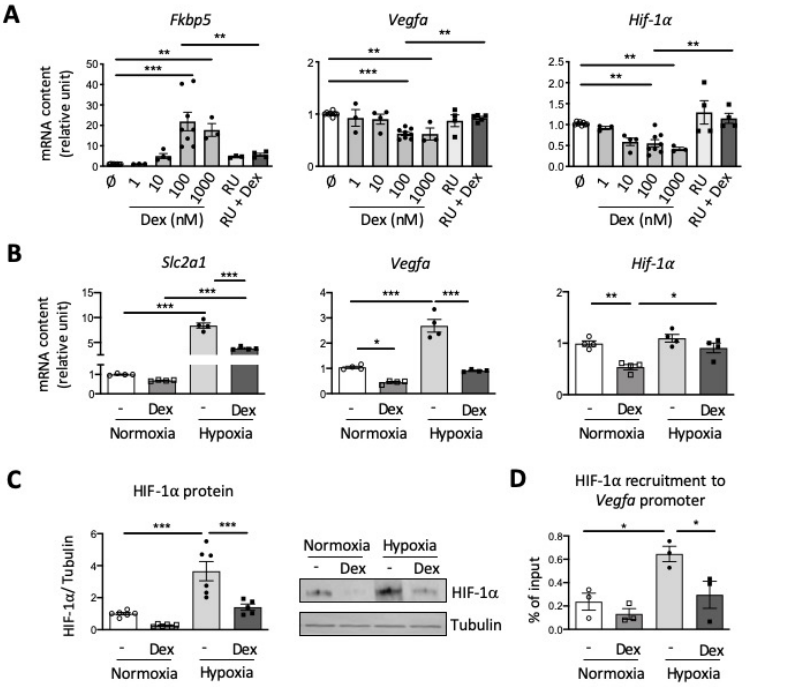

Figure 2. The GR agonist dexamethasone inhibits Vegfa and Hif-1α expression in 3T3-F442A mature adipocytes

3T3-F442A mature adipocytes were treated with the indicated concentrations of the selective-GR agonist dexamethasone (Dex) in the presence or absence of the antagonist RU-486 (RU) during 16 hours. A: Relative gene expression of Fkbp5, Vegfa and Hif-1α was determined in response to different doses of Dex, with or without 100 □M RU-486 (n = 3-8 experiments).

B-D: 3T3-F442A mature adipocytes were placed under normoxic or hypoxic condition, in the presence or absence of 100 nM Dex during 16 hours. (B) Slc2a1, Vegfa and Hif-1α relative gene expression was measured by RT-qPCR (n = 4 experiments). (C) Representative Western blot and quantification of HIF-1α protein (n = 6 experiments). (D) ChIP analysis of HIF-1α binding onto Vegfa promoter. Immunoprecipitation (IP) was conducted with HIF-1α antibody. The DNA region of the Vegfa promoter was amplified by qPCR (n = 3 experiments).

Data are presented as the mean +/- SEM. Each data point represents one experiment performed in triplicate except in panel D where each data point represents one experiment. *P<0.05, **P<0.01 and ***P<0.001,

as determined by Kruskal-Wallis test and one-way ANOVA, followed by the Bonferroni post-hoc test to compare means.

190x275mm (96 x 96 DPI)

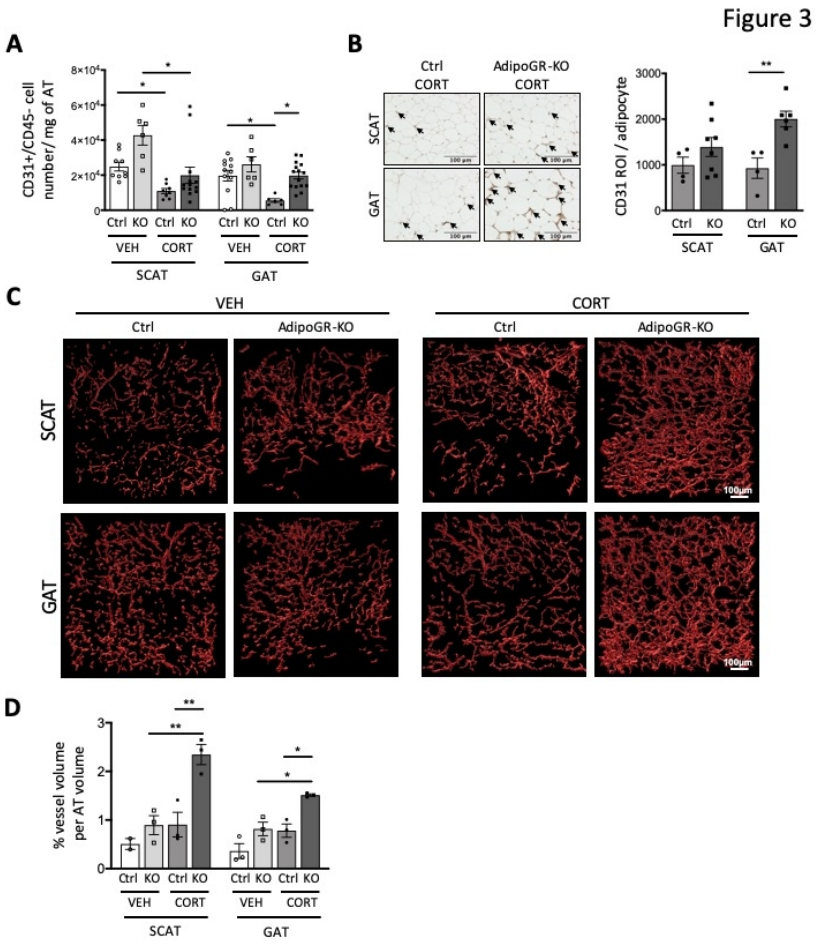

Figure 3. AdipoGR-KO mice exhibit an increased AT vascularization under CORT treatment
Control (Ctrl) and AdipoGR-KO mice were analyzed after a 4-week exposure to VEH or CORT. A: Flow cytometry analysis of endothelial cells was performed on the stromal vascular fraction (SVF) isolated from subcutaneous adipose tissue (SCAT) and gonadal adipose tissue (GAT) of VEH- and CORT-treated animals. Number of CD31+/CD45- endothelial cells in SCAT and GAT was determined per mg of AT (n = 6-16/group). B: Representative pictures of CD31 labeling (pointed by arrows, left panel) on SCAT and GAT sections from CORT-treated Ctrl and AdipoGR-KO mice and quantification (right panel) of CD31 intensity (ROI) per adipocyte (n = 4-8/group). C: Representative perspective 3D projection image of the vasculature in SCAT and GAT of treated mice. Fluorescent (Tomato) lectin was used as a marker of blood vessels in cleared AT. D: Quantification of vasculature as percent of vessel volume per AT volume (n = 2-3/group).
Data are presented as the mean +/- SEM. Each data point represents one animal. *P<0.05 and **P<0.01, as determined by a student's t test, Kruskal-Wallis test and one-way ANOVA, followed by the Bonferroni post-hoc test to compare means.

190x275mm (96 x 96 DPI)

Figure 4

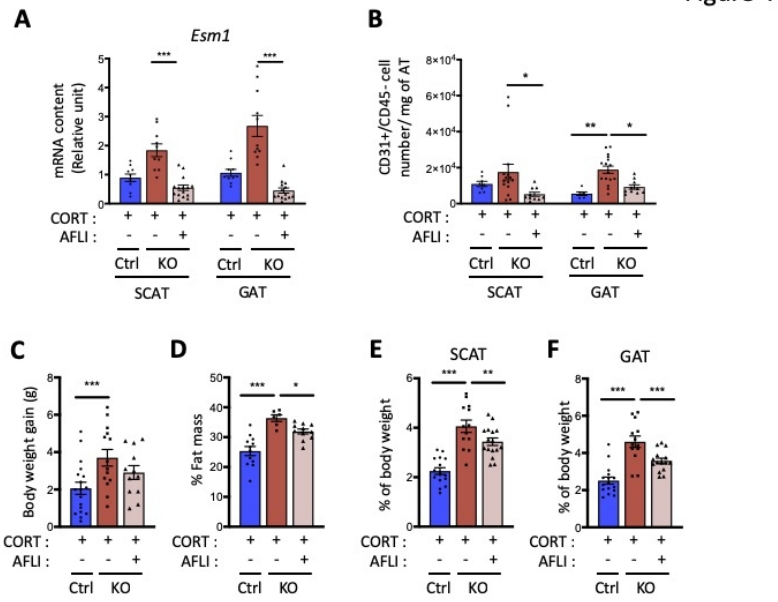

Figure 4. Aflibercept prevents adipose tissue angiogenesis and expansion in CORT-treated AdipoGR-KO mice
Control (Ctrl) and AdipoGR-KO mice were treated with CORT alone or in combination with the soluble decoy receptor, Aflibercept (AFLI) or the diluent (PBS) during 4 weeks. A: Relative gene expression of Esm1 was determined by RT-qPCR in subcutaneous adipose tissue (SCAT) and gonadal adipose tissue (GAT) of Ctrl and AdipoGR-KO mice (n = 10-12/group). B: Flow cytometry analysis of endothelial cells was performed on the stromal vascular fraction (SVF) isolated from SCAT and GAT of CORT-treated mice. Number of CD31+/CD45- endothelial cells in SCAT and GAT was determined per mg of AT (n = 6-16/group). Of note, flow cytometry on AFLI groups were performed simultaneously with the groups presented in Fig. 3A. C: Body weight gain is presented after 4 weeks of treatment (n = 12-18/group). D: Fat body composition was determined by DEXA analyzer (n = 6-12/group). E-F: Subcutaneous adipose tissue (SCAT) and gonadal adipose tissue (GAT) weights are presented as the percentage of total body weight of Ctrl and AdipoGR-KO mice (n = 13-16/group).
Data are presented as the mean +/- SEM. Each data point represents one animal. *P<0.05, **P<0.01 and ***P<0.001, as determined by Kruskal-Wallis test and one-way ANOVA, followed by the Bonferroni post-hoc

test to compare means.
See also Supplementary Fig. 2.

190x275mm (96 x 96 DPI)

Figure 5

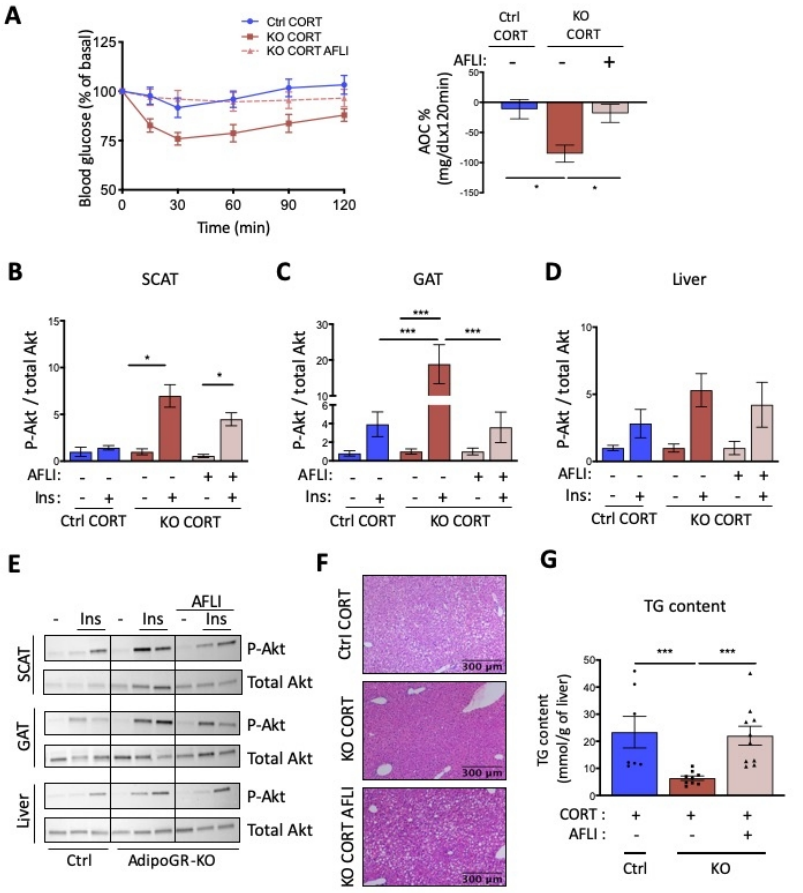

Figure 5. Blocking VEGFA impairs insulin sensitivity in CORT-treated AdipoGR-KO mice
Control (Ctrl) and AdipoGR-KO mice were treated with CORT in combination with the soluble decoy receptor, Aflibercept (AFLI) or its diluent (PBS) during 4 weeks. A: Insulin tolerance test (ITT) was performed on Ctrl and AdipoGR-KO mice fasted for 5 h (n = 10-20/group). Glucose levels were determined at indicated times (left panel) and the area of the curve was determined (AOC, right panel) for each ITT. B-E: Insulin pulses were performed in Ctrl and AdipoGR-KO mice. Quantification of insulin-stimulated phosphorylation of (P-)Akt to total Akt in (B) subcutaneous adipose tissue (SCAT), (C) gonadal adipose tissue (GAT), and (D) liver (n = 3-6/group). (E) Representative cropped Western blots are presented. F: Representative hematoxylin and eosin staining of liver sections of Ctrl and AdipoGR-KO mice. G: Liver triglyceride (TG) content were analyzed (n = 8-10/group).
Data are presented as the mean +/- SEM. *P<0.05, and ***P<0.001, as determined by Kruskal-Wallis test and one-way ANOVA, followed by the Bonferroni post-hoc test to compare means.

190x275mm (96 x 96 DPI)

Figure 6

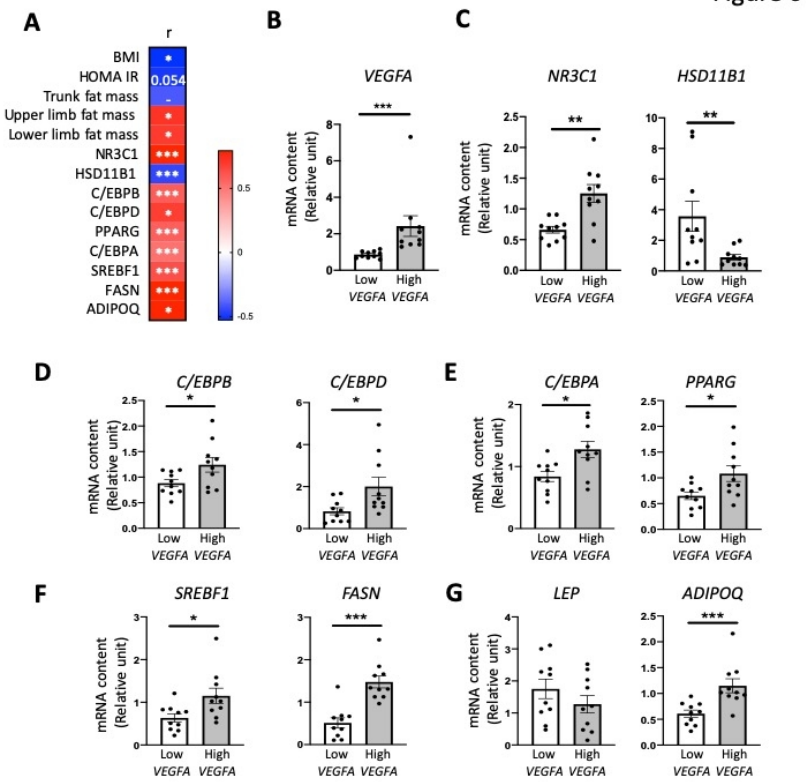

Figure 6. Higher human VEGFA expression in SCAT is associated with healthier metabolic profile

(A) Spearman correlation heatmap indicates correlation between VEGFA expression in the SCAT of patients with Cushing's syndrome (LIPOCUSH cohort) and their clinical, anthropometric and molecular traits. Intensities of blue and red colors indicate values of positive and negative correlation coefficients, respectively Rho correlations and P values are detailed in the figure and in the Supplementary Table 5. *P<0.05, **P<0.01 and ***P<0.001.

(B-G) Twenty patients with Cushing's syndrome were divided into two subgroups according to their lowest and highest levels of VEGFA expression in SCAT, based on the stratified median of VEGFA gene expression. The two subgroups (low and high VEGFA expression) were compared to each other in term of gene expression of (B) VEGFA, (C) NR3C1 and HSD11B1, (D) early (C/EBPB, C/EBPD), and (E) late (C/EBPA and PPARG) adipogenic transcription factors, (F) lipogenic markers (SREBF1 and FASN) and (G) adipokines (LEP and ADIPOQ), (n = 10 patients/group).

Each data point represents one patient. Data are presented as the mean +/- SEM. *P<0.05, **P<0.01 and ***P<0.001, as determined by Student's t Welch and Mann-Whitney test to compare means.

See also Supplementary Tables 3 and 4.

190x275mm (96 x 96 DPI)

Online Supplemental Material

Adipocyte glucocorticoid receptor impairs adipose tissue healthy expansion through repression of angiogenesis

Anna Vali[1,2], Héloïse Dalle[1,2], Jérôme Gilleron[3], Emmanuelle Havis[4], Marie Garcia[1,2], Carine Beaupère[1,2], Clémentine Denis[1,2], Natacha Roblot[1,2], Karine Poussin[1,2], Tatiana Ledent[1], Benjamin Bouillet[1,2], Mireille Cormont[3], Jean-François Tanti[3], Jacqueline Capeau[1,2], Camille Vatier[2,5], Bruno Fève[2,5]*, Alexandra Grosfeld[1,2]*, Marthe Moldes[1,2#]

Affiliations

[1]Sorbonne Université, Inserm, Centre de Recherche Saint-Antoine, CRSA, F-75012 Paris, France
[2]Sorbonne Université, Inserm, Institute of CardioMetabolism and Nutrition, ICAN, F-75013 Paris, France
[3]Université Côte d'Azur, Inserm, C3M, Team Cellular and Molecular Pathophysiology of Obesity, Nice, France
[4]Sorbonne Université, CNRS, Inserm, Laboratoire de Biologie du Développement, Institut Biologie Paris Seine, IBPS, F75005 Paris, France
[5]Sorbonne Université, Inserm, Centre de Recherche Saint-Antoine, CRSA, AP-HP, Hôpital Saint-Antoine, Service Endocrinologie, CRMR PRISIS, 75012 Paris, France

*These authors contributed equally.

#Correspondence should be addressed to marthe.moldes@inserm.fr

Supplemental Methods

Animals and treatments

All animals were housed with a 12 h light/dark cycle and had free access to water and standard chow diet (LASQCdiet® Rod16-R, LASvendi, Soest, Germany). Cre recombinase was activated in 10-week-old male mice by intraperitoneal injection of tamoxifen (60 mg/g/day) (MP Biomedicals, Illkirch-Graffenstaden, France) for 5 consecutive days. Fourteen-week-old AdipoGR-KO and GR-Flox control littermate (hereafter defined as Ctrl) mice were treated for 4 days or 4 weeks with corticosterone (CORT, 100 μg/mL) (Sigma-Aldrich, St. Louis, MO) or vehicle (VEH) (1% ethanol) added to drinking water (1). For the VEGFA blockade experiment, the soluble decoy receptor Aflibercept (AFLI, 4 mg/kg; Sanofi, Gentilly, France) or diluent (PBS) was injected intraperitoneally twice a week throughout the CORT or VEH treatment for 4 weeks. At sacrifice, tissues were snap-frozen in liquid nitrogen, and kept at -80°C. Blood was drawn by intracardiac puncture with heparin-moistened syringes. Plasma was obtained after centrifugation at 5,000 x *g* for 10 min at 4°C.

Body mass composition was measured using an EchoMRI 100 Whole Body Composition Analyzer (EchoMRI, Houston, TX) according to the manufacturer's instructions.

Cell culture

3T3-F442A preadipocytes were maintained in DMEM high glucose (ThermoFisher Scientific, Montigny-le-Bretonneux, France) with penicillin (100 U/mL) and streptomycin (100 μg/mL) (Sigma–Aldrich, Saint Quentin Fallavier; France) supplemented with 10% bovine calf serum (Dutscher, Issy-les-Moulineaux, France) at 37°C in a 5% CO_2 humidified atmosphere. Differentiation was induced in DMEM supplemented with 10% fetal calf serum (Dutscher) and 1 μM of bovine insulin (Sigma-Aldrich) renewed every other day until total differentiation (day

10). The day before the experiment, mature adipocytes were starved in DMEM with 0.1 % BSA (bovine serum albumin, Sigma-Aldrich) during 24 h before dexamethasone treatment.

RNA extraction and RT-qPCR analysis

Total RNA from human and murine tissues and adipocyte / SVF fractions were purified by Qiazol extraction and purification using Qiagen RNeasy minicolumns according to the manufacturer's instructions (Qiagen, Courtaboeuf, France). 3T3-F442A adipocytes were directly lyzed in RLT buffer of Qiagen RNeasy minicolumns kit as recommended by manufacturer (Qiagen). One μg of total RNA was reverse-transcribed using the High Capacity cDNA Reverse Transcription kit (Applied Biosystems, Foster City, CA, USA). cDNA was amplified using specific primers and the SYBR Green PCR Master mix (Applied Biosystems) according to manufacturer's instructions, using a QuantStudio1 system (ThermoFisher Scientific, Montigny-le-Bretonneux, France). Relative gene expression was determined as arbitrary unit as the ratio of target transcripts to reference genes, Acidic ribosomal phosphoprotein P0/ Ribosomal protein lateral stalk subunit P0 (*36B4/Rplp0*) and Hypoxanthine-guanine phosphoribosyltransferase (*Hprt*) in murine samples and, *RPLP0*, Glyceraldehyde-3-Phosphate Dehydrogenase (*GAPDH*) and Peptidylpropyl Isomerase A (*PPIA*) in human samples. All primer sequences are available in the Supplementary Table 2.

Protein extraction and analysis

Cultured cells, mouse liver and AT were solubilized as previously described (1). Equal protein amounts (20 μg) were separated by SDS-PAGE, transferred onto nitrocellulose membrane and immunodetected with antibodies (Supplementary Table 1). α-tubulin was used to normalize expression. The immunoreactive bands were revealed using the ECL detection kit (Pierce ECL Western Blotting substrate, Rockford, IL, USA) and analyzed using an iBright system

(ThermoFisher, Montigny-le-Bretonneux, France). Ratio P-Akt/total-Akt was quantified using an ImageJ software (Chemi Genius2 scan, GeneSnap; Syngene, Cambridge, UK). VEGFA protein content was measured on adipose tissue extracts with the Quantikine ELISA mouse VEGF kit (R&D systems, Lille, France).

Chromatin Immunoprecipitation (ChIP)

Mature 3T3-F442A adipocytes treated with 100 nM dexamethasone under normoxic or hypoxic condition for 16 hours were homogenized using a mechanical disruption device (Lysing Matrix A, Fast Prep MP1, 3 × 40 sec, MP Biomedicals, Illkirch-Graffenstaden, France). Sonicated chromatin (15 µg) was isolated before chromatin immunoprecipitation and used as positive control for the PCR experiments (input) as previously described in (2). Twenty µg of sonicated chromatin were incubated with 1 µg of rabbit polyclonal anti-HIF-1α (ab1) antibody, or 10 µg of chicken anti-GFP antibody (a negative control), or 10 µg of rabbit polyclonal anti-histone H4 acetylated antibody (a positive control) for immunoprecipitation (Supplementary Table 1). The IP were performed using the ChIP assay kit (Upstate Biotechnology). The DNA was purified using the Nucleospin Gel and PCR Clean Up kit (Qiagen). ChIP products and inputs were then analyzed by quantitative SYBR-green real-time PCR, using primers described in the Supplementary Table 2. All cycle threshold (Ct) values were compared with the input amounts to normalize for variations and presented as fold-enrichment.

AT clearing and 3D-fluorescence imaging

After DyLight 649 labeled Lycopersicon Eculentum (Tomato) lectin staining, SCAT and GAT were collected and fixed in 4% paraformaldehyde (PFA) (pH=7) overnight at 4°C (Supplementary Table 1) and as previously described (3). Briefly, AT were permeabilized, stained with Phalloidin-alexa488 and dehydrated in increasing bath of ethanol. AT were cleared

in methyl-salicylate for at least 2 hours and imaged in an imaging chamber filled with methyl-salicylate using a Nikon A1R-confocal microscope equipped with a 20x long distance objective (C3M imaging facility, Nice, France). 3D stacks were acquired and a pipeline of image post-processing was applied using “bleach correction” and “Gaussian blur” imageJ plugins. 3D images were loaded in IMARIS software. Adipocytes were segmented by using phalloidin staining, vessels were segmented by using lectin staining, and the whole tissue volume were segmented using phalloidin staining. The volume of the vessels and of the whole tissue was obtained using IMARIS statistics. When noticed, these values were reported to the whole tissue volume estimated at sacrifice. Analysis and 3D Volume rendering movies were generated with IMARIS software.

Patients with Cushing’s syndrome

Patients underwent unilateral adrenalectomy allowing, at the same time, biopsies of SCAT. Between 2010 and 2015, twenty patients were recruited by the Endocrinology Departments of the University Hospital centers of Saint-Antoine, Cochin, Pitié Salpêtrière (Paris), Bicêtre (Kremlin-Bicêtre), Henri Mondor (Créteil) and Haut-Lévêque (Bordeaux). Dual energy X-ray absorptiometry (DEXA) was performed to evaluate lean and fat mass body compositions at trunk, lower and upper limbs. Collection of clinical data and blood samples (5 mL) were carried out under appropriate conditions. Approximately 200 mg of SCAT was collected for each patient and stored in liquid nitrogen. SCAT and other metabolic parameters were compared between two subgroups of Cushing patients, determined according to the value of *VEGFA* expression, giving a "low *VEGFA* expressing" group and a "high *VEGFA* expressing" group. The clinical, biological and anthropometric data of Cushing patients are reported in Supplementary Tables 3 and 4.

Study approval

All experiments were carried out according to the European Communities Council Directive (2010/63/UE) for the care and use of animals for experimental procedures and complied with the regulations of the French Ethics Committee in Animal Experiment « Charles Darwin » (Ile-de-France, Paris, n°5). All procedures were approved by this committee (n° #4625-2016032111413252v2 and 18442-201901141010547v1). For the human study, the LIPOCUSH cohort, whose National Clinical Trial (NCT) number is NCT01688349, was funded by an AP-HP Clinical Research Contract, and required the consent of all patients prior to participation.

References

1. Dalle H, Garcia M, Antoine B, Boehm V, Do T, Buyse M, Ledent T, Lamazière A, Magnan C, Postic C, Denis R, Luquet S, Fève B, Moldes M. Adipocyte Glucocorticoid Receptor Deficiency Promotes Adipose Tissue Expandability and Improves the Metabolic Profile Under Corticosterone Exposure. Diabetes. 2019;68: 305-317
2. Milet C, Bléher M, Allbright K, Orgeur M, Coulpier F, Duprez D, Havis E. Egr1 deficiency induces browning of inguinal subcutaneous white adipose tissue in mice. Sci Rep. 2017;7:16153
3. Gilleron J, Meziat C, Sulen A, Ivanov S, Jager J, Estève D, Muller C, Tanti J, Cormont M. Exploring Adipose Tissue Structure by Methylsalicylate Clearing and 3D Imaging. J Vis Exp. 2020;162

Supplementary Table 1: List of antibodies

Experiment	Antibodies	Reference	Company	Dilution or concentration
IHC	Monoclonal anti-CD31	# sc-53411	Santa Cruz Biotechnology, Germany	1:50
	Secondary antibody biotinylated	# RPN 1001	Amersham, Les Ulis, France	1:5000
	Streptavidine-HRP	# 016-030-084	Jackson Immuno Research, Cambridgeshire, UK	1:100
FACS	Alexa-Fluor® 488 anti-mouse CD45	#160306	BioLegend, London, UK	1.25 µg/µl
	Alexa-Fluor® 488 rat IgG2a, κ isotype control	#400525	BioLegend, London, UK	1.25 µg/µl
	Brilliant Violet™ 421 anti-mouse CD31	#102424	BioLegend, London, UK	1.25 µg/µl
	Brilliant Violet™ 421 rat IgG2a, κ isotype control	#400549	BioLegend, London, UK	1.25 µg/µl
3D fluorescence imaging	DyLight 649 Lycopersicon Esculentum Lectin	#DL-1178-1	Vector Laboratories Burlingame, USA	2 µg/µl
WB	Rabbit polyclonal anti-Phospho-Akt (Ser 473)	# 9271L	Cell Signaling Technology, Danvers, MA, USA	1:1000
	Rabbit polyclonal anti-Akt	# 9272S	Cell Signaling Technology, Danvers, MA, USA	1:1000
	Rabbit polyclonal anti-HIF-1α	# NB100-449	Bio-Techne Ltd., Abingdon, UK	1:500
	Monoclonal anti α-tubulin	#T5168	Sigma-Aldrich, Saint Quentin Fallavier; France	1:10,000
	Anti-rabbit IgG HRP-linked	#7074S	Cell Signaling Technology, Danvers, MA, USA	1:5000
	Anti-mouse IgG HRP-linked	#7076S	Cell Signaling Technology, Danvers, MA, USA	1:5000
ChIP	Rabbit polyclonal anti-HIF-1α	# NB100-449	Bio-Techne Ltd., Abingdon, UK	1:200
	Chicken polyclonal anti-GFP	# GFP 1020	Interchim, Montluçon France	1:1000
	Rabbit polyclonal anti-Histone H4a	# 06-866	Sigma-Aldrich, France	1:100

Supplementary Table 2: List of murine and human primers for RT-qPCR and ChIP analysis

Gene	Forward primers	Reverse primers
Mouse 36b4	5'-GCTGATGGGCAAGAACACCA-3'	5'-CCCAAAGCCTGGAAGAAGGA-3'
Mouse Hprt	5'-AGGACCTCTCGAAGTGT-3'	5'-TCAAATCCCTGAAGTACTCAT-3'
Mouse Gr	5'-GGGCGCCAAGTGATTGCCGCAGT-3'	5'-CCAACCCAGGGCAAATGCCATGA-3'
Mouse Fkbp5	5'-TGTTCAAGAAGTTCGCAGAGC-3'	5'-CCTTCTTGCTCCCAGCTTT-3'
Mouse Vegfa	5'-AAAAACGAAAGCGCAAGAAA-3'	5'-TTTCTCCGCTCTGAACAAAGG-3'
Mouse Hif-1α	5'-GCACTAGACAAAGTTCACCTGAGA-3'	5'-CGCTATCCACATCAAAGCAA-3'
Mouse Slc2a1	5'-CCACAGTGAAGGCCGTGTT-3'	5'-GGTATCAATGCTGTGTTCTACTACTACA-3'
Mouse Esm1	5'-CAGTATGCAGCAGCCAAATC-3'	5'-GATGCTGAGTCACGCTCTGT-3'
HRE-containing murine Vegfa promoter	5'-CGAGGGTTGGCGGCAGGAC-3'	5'-CAGTGGCGGGGAGTGAGACG-3'
Human RPLP0	5'-GGCGACCTGGAAGTCCAACT-3'	5'-CCATCAGCACCACAGCCTTC-3'
Human GAPDH	5'-AGCCACATCGCTCAGACAC-3'	5'-GCCCAATACGACCAAATCC-3'
Human PPIA	5'-ATGCTGGACCCAACACAAAT-3'	5'-TCTTTCACTTTGCCAAACACC-3'
Human VEGFA	5'-TGCCGCCACACCATCAC-3'	5'-GTCTCGCCCTCCGGACCCAA-3'
Human NR3C1	5'-CCTTCTGCGTTCACAAGCTA-3'	5'-TTCTTTGGAGTCCATCAGTGAAT-3'
Human HSD1B11	5'-TCTGTGTTCTTGGCCTCATAGA-3'	5'-GAGCTGCTTGCATATGGACTATC-3'
Human C/EBPB	5'-TGCTTGAACAAGTTGGGCAG-3'	5'-GCGCGAGCGCAACAACA-3'
Human C/EBPD	5'-GGACATAGGAGCGCAAAGAA -3'	5'-GCTTCTCTCGCAGTTTAGTGG-3'
Human C/EBPA	5'-GACATCAGCGCCTACATCG-3'	5'-GGCTGTGCTGGAACAGGT-3'
Human PPARG	5'-CTCATATCCGAGGGCCAA-3'	5'-TGCCAAGTCGCTGTCATC-3'
Human SREBF1C	5'-GGAGGGGTAGGCCAACGGCCT-3'	5'-CATGTCTTCGAAAGTGCAATCC-3'
Human FASN	5'-CAGGCACACACGATGGAC-3'	5'-CGGAGTGAATCTGGGTTGAT-3'
Human Leptin	5'-TTGTCACCAGGATCAATGACA-3'	5'-GTCCAAACCGGTGACTTTCT-3'
Human Adiponectin	5'-GGTGAGAAGGGTGAGAAAGGA-3'	5'-TTTCACCGATGTCTCCCTTAG-3'

Supplementary Table 3. Relationship between *VEGFA* gene expression and clinical and biological parameters of patients with Cushing's syndrome

Twenty patients with a Cushing's syndrome related to a cortisolic adenoma (LIPOCUSH cohort) were divided in two subgroups according to their lowest and highest levels of *VEGFA* expression in SCAT, based on the stratified median of *VEGFA* gene expression (10 per group, unless indicated). Data are presented as the mean +/- SD. *P<0.05, as determined by Student's t Welch and Mann-Whitney tests to compare means. (HOMA-IR: homeostasic model assessment of insulin resistance, HbA1c: glycated hemoglobin A1c, TG: triglycerides, FFA: free fatty acids)

Biological parameters	All patients with Cushing's syndrome	Patients with the lowest VEGFA expression in SCAT	Patients with the highest VEGFA expression in SCAT	*P*-value
Total number	20	10	10	-
Gender (M/F)	2/18	1/9	1/9	-
Age (years) (*n=20*)	46.4 ± 14.2	50.3 ± 12.2	42.5 ± 15.5	*P=0.228*
Midnight cortisol levels (µg/dL) (*n=15*)	19 ± 12.7	19.9 ± 17.4	18.2 ± 7.8	*P=0.444*
Serum cortisol levels after 1 mg Dex (µg/dL) (*n=15*)	18 ± 11	15.7 ± 12.2	20.7 ± 9.5	*P=0.394*
Free urinary Cortisol (nmol/24h) (*n=18*)	423.7 ± 442	293.1 ± 261.2	587 ± 576	*P=0.360*
HOMA-IR (*n=15*)	3.1 ± 4.3	5.3 ± 5.9	1.3 ± 0.8	*P=0.029**
HbA1c (%) (*n=16*)	6.5 ± 1.5	7.1 ± 1.7	5.7 ± 0.6	*P=0.037**
TG (mmol/L) (*n=14*)	2.2 ± 2.0	2.1 ± 1.5	2.4 ± 2.6	*P=0.950*
FFA (mmol/L) (*n=20*)	0.62 ± 0.20	0.64 ± 0.23	0.62 ± 0.19	*P=0.837*

Supplementary Table 4. Relationship between *VEGFA* gene expression and anthropometric parameters of patients with Cushing's syndrome

Eleven patients of the LIPOCUSH cohort underwent DEXA analysis to determine body fat repartition. We divided them into two subgroups according to their lowest (n = 4) and highest (n = 7) levels of *VEGFA* expression as in Supplementary Table 3. Data are presented as the mean +/- SD. *P<0.05, as determined by Student's t Welch and Mann-Whitney tests to compare means.

Anthropometric parameters	All patients with Cushing's syndrome	Patients with the lowest VEGFA expression in SCAT	Patients with the highest VEGFA expression in SCAT	*P*-value
BMI (kg/m^2)	30.0 ± 7.7	36.2 ± 9.3	26.4 ± 3.9	*P=0.123*
Total fat mass (kg)	38.9 ± 15.4	44.1 ± 17.5	36.0 ± 15.0	*P=0.465*
Total fat mass (% of total body mass)	43.4 ± 9.2	42.4 ± 11.9	43.9 ± 8.4	*P=0.827*
Upper limb fat mass (% of upper limb mass)	23.7 ± 16.4	12.7 ± 4.6	29.9 ± 17.6	*P=0.043**
Lower limb fat mass (% of lower limb mass)	36.2 ± 12.7	26.7 ± 5	41.6 ± 12.8	*P=0.021**
Trunk fat mass (% of trunk mass)	48.9 ± 9.9	50.7 ± 13.3	47.9 ± 8.4	*P=0.726*

Supplementary Table 5. Correlation between *VEGFA* expression and clinical, anthropometric and molecular traits of patients with Cushing's syndrome

Correlations (Spearman's test) were performed between *VEGFA* expression and clinical, anthropometric parameters (n=11-15), and adipocyte-related gene expression in SCAT (determined by RT-PCR; n=20) from patients with Cushing's syndrome (LIPOCUSH cohort). (HOMA-IR: homeostasic model assessment of insulin resistance, BMI: body mass index).

		VEGFA	
		r	*P*
Clinical parameter	HOMA-IR	-0.494	*0.054*
Anthropometric parameters	BMI	-0.527	*0.017*
	Trunk fat mass	-0.409	*0.214*
	Upper limb fat mass	0.715	*0.016*
	Lower limb fat mass	0.691	*0.023*
GC signaling pathway markers	*NR3C1*	0.777	*5.49E-05*
	HSB11B1	-0.451	*0.046*
Adipogenic markers	*C/EBPB*	0.580	*0.007*
	C/EBPD	0.683	*0.001*
	PPARG	0.571	*0.008*
	C/EBPA	0.517	*0.020*
Lipogenic markers	*SREBF1*	0.624	*0.003*
	FASN	0.792	*3.10E-05*
Adipokine	*ADIPOQ*	0.785	*4.15E-05*

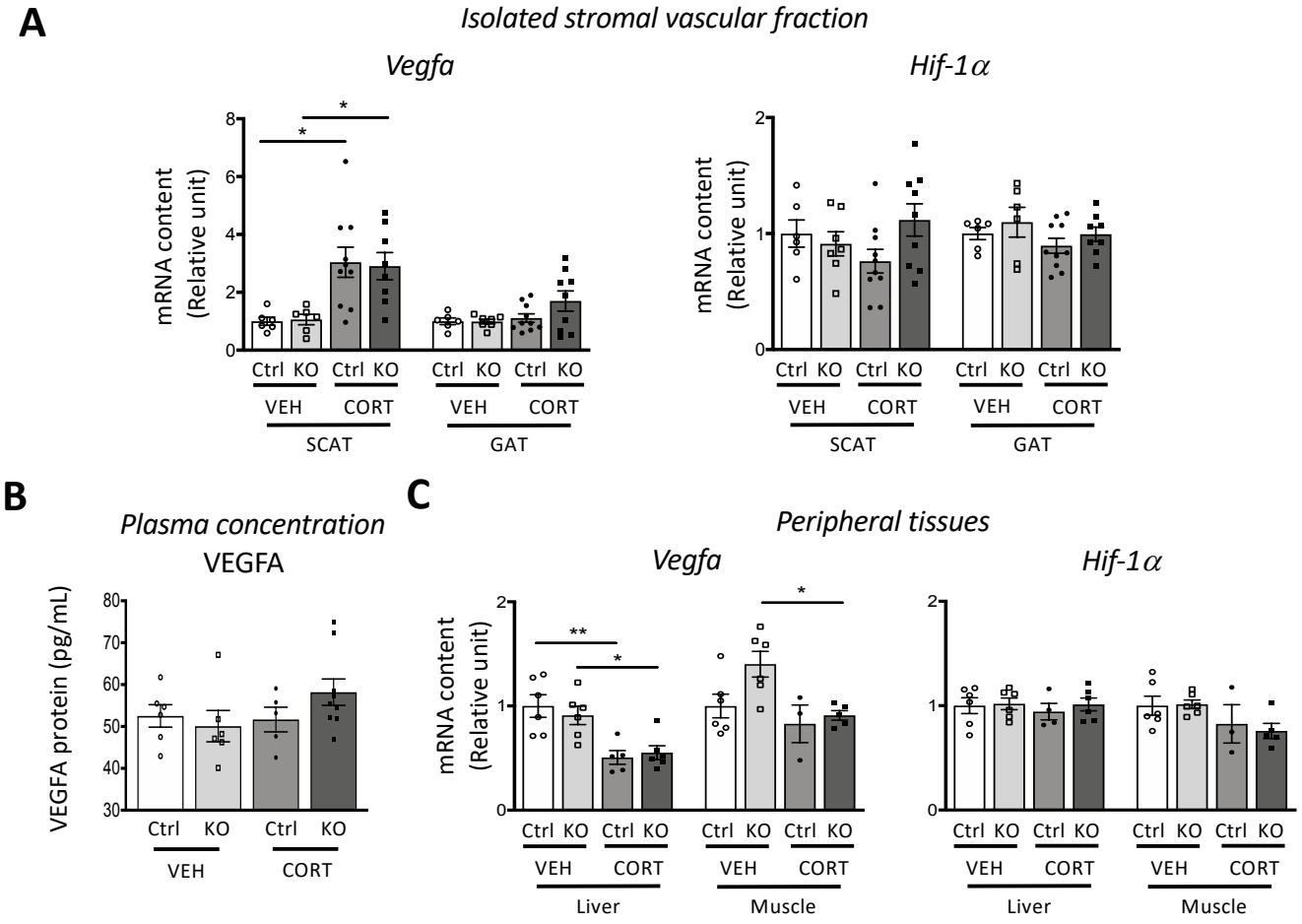

Supplementary Figure 1. Expression of Vegfa and Hif-1a in adipocyte-specific Gr-deficient mice treated with VEH or CORT. Related to Fig. 1.

Control (Ctrl) and AdipoGR-KO mice were analyzed after 4 weeks of exposure with VEH or CORT. A: Relative gene expression was determined by RT-qPCR for Vegfa and Hif-1α mRNA content in the stromal vascular fraction (n = 6-10/group) isolated from SCAT and GAT. B: VEGFA protein concentration was measured in plasma samples of VEH- and CORT-treated Ctrl and AdipoGR-KO mice (n = 5-9/group). C: Vegfa and Hif-1α mRNA expression was determined by RT-qPCR in the liver and muscle of mice (n = 3-6/group). Data are presented as the mean +/- SEM. Each data point represents one animal. *P<0.05, **P<0.01, as determined by one-way ANOVA, followed by the Bonferroni post-hoc test to compare means.

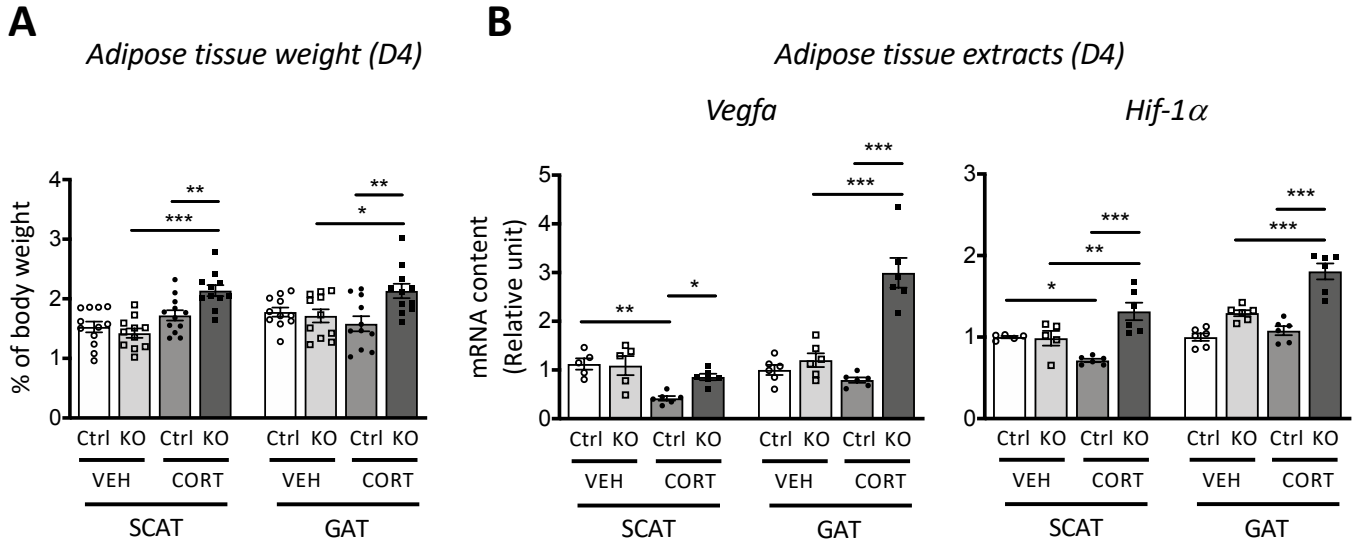

Supplementary Figure 2. AdipoGR-KO mice display an enhanced body weight and expression of Vegfa and Hif-1α from 4 days of CORT treatment. Related to Fig. 1

Control (Ctrl) and AdipoGR-KO mice were analyzed at day 4 (D4) of VEH or CORT treatment. A: Subcutaneous adipose tissue (SCAT) and gonadal adipose tissue (GAT) weights are presented as the percentage of total body weight of Ctrl and AdipoGR-KO mice (n = 11-12/group). B: Relative gene expression of Vegfa and Hif-1α was determined by RT-qPCR in SCAT and GAT (n = 5-6/group). Data are presented as the mean +/- SEM. Each data point represents one animal. *P<0.05, **P<0.01 and ***P<0.001, as determined by one-way ANOVA, followed by the Bonferroni post-hoc test to compare means.

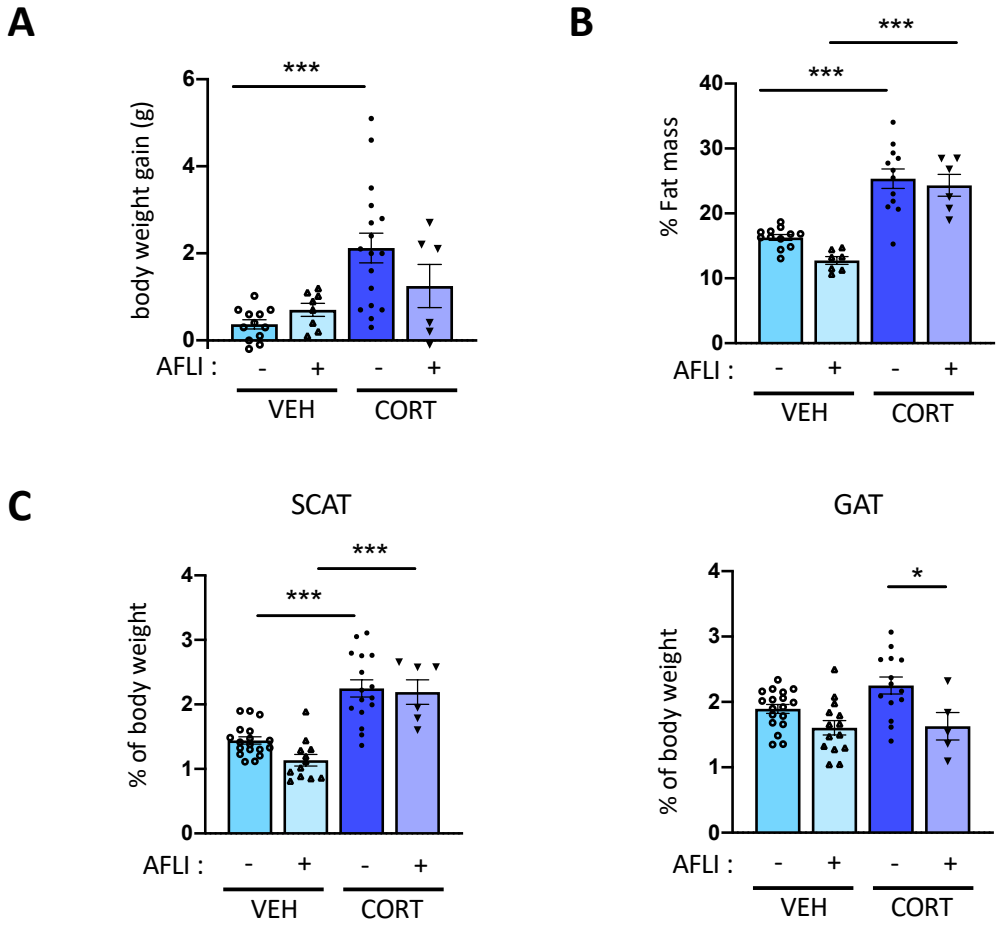

Supplementary Figure 3. Effect of Aflibercept treatment on VEH- and CORT-treated control mice. Related to Fig. 4.

Control (Ctrl) mice were treated with VEH or CORT alone, or in combination with the soluble decoy receptor, Aflibercept (AFLI) or the vehicle solution (PBS) during 4 weeks. A: Body weight gain is presented after 4 weeks of treatment (n = 6-17/group). B: Fat body composition was determined by DEXA analyzer (n = 6-12/group). C: SCAT and GAT weights are presented as the percentage of total body weight of Ctrl mice (n = 5-18/group). Data are presented as the mean +/- SEM. Each data point represents one animal. *P<0.05 and ***P<0.001 as determined by one-way ANOVA, followed by the Bonferroni post-hoc test to compare means.

Supplemental Movies

Supplementary Movie 1. SCAT vascular network of VEH-treated control mice

Supplementary Movie 2. SCAT vascular network of VEH-treated AdipoGR-KO mice

Supplementary Movie 3. SCAT vascular network of CORT-treated control mice

Supplementary Movie 4. SCAT vascular network of CORT-treated AdipoGR-KO mice

Supplementary Movie 5. GAT vascular network of VEH-treated control mice

Supplementary Movie 6. GAT vascular network of VEH-treated AdipoGR-KO mice

Supplementary Movie 7. GAT vascular network of CORT-treated control mice

Supplementary Movie 8. GAT vascular network of CORT-treated AdipoGR-KO mice